

DTIC FILE COPY

AD-A234 978



2

NAVAL POSTGRADUATE SCHOOL Monterey, California

~~AD-A234 978~~



THESIS

DTIC
ELECTE
MAYO 1 1991
S B D

ESTABLISHMENT OF A REMOTELY PILOTED HELICOPTER
TEST FLIGHT PROGRAM
FOR HIGHER HARMONIC CONTROL RESEARCH

by

James Georg Scott

June 1990

Thesis Advisor:

E. Roberts Wood

Approved for public release; distribution is unlimited

DTIC FILE COPY

BEST
AVAILABLE COPY

~~91 1 20 057~~

91 5 01 002

Unclassified

Security Classification of this page

REPORT DOCUMENTATION PAGE

1a Report Security Classification UNCLASSIFIED		1b Restrictive Markings	
2a Security Classification Authority		3 Distribution Availability of Report	
2b Declassification/Downgrading Schedule		Approved for public release; distribution is unlimited	
4 Performing Organization Report Number(s)		5 Monitoring Organization Report Number(s)	
6a Name of Performing Organization	6b Office Symbol	7a Name of Monitoring Organization	
Naval Postgraduate School	(If Applicable) AA	Naval Postgraduate School	
6c Address (city, state, and ZIP code)		7b Address (city, state, and ZIP code)	
Monterey, CA 93943-5000		Monterey, CA 93943-5000	
8a Name of Funding/Sponsoring Organization	8b Office Symbol	9 Procurement Instrument Identification Number	
	(If Applicable)		
8c Address (city, state, and ZIP code)		10 Source of Funding Numbers	
		Program Element Number	Project No
		Task No	Work Unit Accession No
11 Title (Include Security Classification) ESTABLISHMENT OF A REMOTELY PILOTED HELICOPTER TEST FLIGHT PROGRAM FOR HIGHER HARMONIC CONTROL RESEARCH			
12 Personal Author(s) Scott, James, G.			
13a Type of Report	13b Time Covered	14 Date of Report (year, month, day)	15 Page Count
Master's Thesis	From To	June 1990	72
16 Supplementary Notation The views expressed in this thesis are those of the author and do not reflect the official policy or position of the Department of Defense or the U.S. Government.			
17 Cosati Codes		18 Subject Terms (continue on reverse if necessary and identify by block number)	
Field	Group	Subgroup	
		HHC, RPH, UAV, RPV, Vibration, Controls, Torsional Constant, Freeplay	
19 Abstract (continue on reverse if necessary and identify by block number)			
<p>The Department of Aeronautics and Astronautics at the Naval Postgraduate School (NPS) has begun analytical research of a helicopter vibration reduction concept known as higher harmonic control (HHC). To supplement this research, a helicopter flight test program has been established to generate flight test data in support of the NPS HHC research efforts. To accomplish this task, a remotely piloted helicopter has been chosen as the test vehicle. The research efforts encompassed by this thesis are the determination of attributes required of a RPH used for HHC studies, the selection and acquisition of an RPH capable of completing the intended research mission, and the preliminary analysis of the RPH's flight control system for modification to an HHC configuration. A brief overview of helicopter vibrations and HHC fundamentals, along with an in-depth description of the selected RPH, is presented. The preliminary analysis of the RPH's flight control system includes the determination of associated freeplay and torsional constant values for the flight control components and the calculation of the necessary actuator torque requirements for HHC actuation. This research effort is the first stage of a long term program designed to provide NPS with an inhouse asset capable of generating HHC flight test data in support of analytical research. 25</p>			
20 Distribution/Availability of Abstract		21 Abstract Security Classification	
<input checked="" type="checkbox"/> unclassified/unlimited <input type="checkbox"/> same as report <input type="checkbox"/> DTIC users		UNCLASSIFIED	
22a Name of Responsible Individual		22b Telephone (Include Area code)	22c Office Symbol
E. Roberts Wood		(408) 646-2311	Code AA

DD FORM 1473, 84 MAR

83 APR edition may be used until exhausted

security classification of this page

All other editions are obsolete

Unclassified

* Helicopters, * Vibration, * Harmonics,
 HHC (Higher Harmonic Control), Thesis. →

Approved for public release; distribution is unlimited.

Establishment of a Remotely Piloted Helicopter
Test Flight Program
for Higher Harmonic Control Research

by

James Georg Scott
Lieutenant, United States Navy
B.S., The Pennsylvania State University, 1982

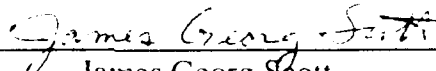
Submitted in partial fulfillment of the
requirements for the degree of

MASTER OF SCIENCE IN AERONAUTICAL ENGINEERING

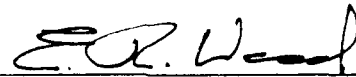
from the

NAVAL POSTGRADUATE SCHOOL
June 1990

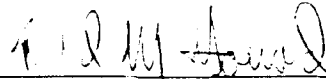
Author:


James Georg Scott

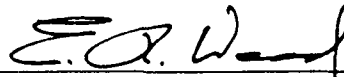
Approved by:



E. Roberts Wood, Thesis Advisor



Richard M. Howard, Second Reader



E. Roberts Wood, Chairman,
Department of Aeronautics and Astronautics

ABSTRACT

The Department of Aeronautics and Astronautics at the Naval Postgraduate School (NPS) has begun analytical research of a helicopter vibration reduction concept known as higher harmonic control (HHC). To supplement this research, a helicopter flight test program has been established to generate flight test data in support of the NPS HHC research efforts. To accomplish this task, a remotely piloted helicopter (RPH) has been chosen as the test vehicle. The research efforts encompassed by this thesis are the determination of attributes required of a RPH used for HHC studies, the selection and acquisition of an RPH capable of completing the intended research mission, and the preliminary analysis of the RPH's flight control system for modification to an HHC configuration. A brief overview of helicopter vibrations and HHC fundamentals, along with an in-depth description of the selected RPH, is presented. The preliminary analysis of the RPH's flight control system includes the determination of associated freeplay and torsional constant values for the flight control components and the calculation of the necessary actuator torque requirements for HHC actuation. This research effort is the first stage of a long term program designed to provide NPS with an inhouse asset capable of generating HHC flight test data in support of analytical research.

Accession For	
NTIS GRA&I	<input checked="" type="checkbox"/>
DTIC TAB	<input type="checkbox"/>
Unannounced	<input type="checkbox"/>
Justification	
By	
Distribution/	
Availability Codes	
Dist	Avail and/or Special
A-1	

I.	INTRODUCTION.....	1
II.	SCOPE.....	3
III.	BACKGROUND.....	5
	A. PRINCIPLES OF HIGHER HARMONIC CONTROL.....	5
	1. The Origin of Helicopter Vibrations.....	5
	2. Higher Harmonic Control Inputs.....	6
IV.	RPH DEFINITION, ACQUISITION, AND SUPPORT.....	8
	A. DEFINITION OF A SUITABLE RPH.....	8
	B. ACQUISITION OF THE RPH.....	9
	C. RPH SUPPORT REQUIREMENTS.....	9
	1. Laboratory Facility.....	9
	2. Flying sites.....	10
	3. Piloting of the RPH.....	10
V.	THE REMOTELY PILOTED HELICOPTER SYSTEM.....	12
	A. AIRCRAFT DESCRIPTION.....	12
	1. Airframe.....	14
	2. Rotor System.....	15
	3. Flight Control System.....	17
	4. Radio System.....	21
	5. Electrical System.....	26
	6. Powerplant	27
	7. Telemetry Equipment.....	31
VI.	HIGHER HARMONIC CONTROL MODIFICATIONS.....	34
	A. CONTROL SYSTEM FREEPLAY AND TORSIONAL CONSTANTS.....	35
	1. Servo Actuator Assembly.....	37
	2. Blade Pitch Link and Pitch Horn Assembly.....	38
	3. Total System	39
	4. Comparison of Individual Spring Constant Data.....	41

B. BLADE FLAPPING HINGE TORSIONAL CONSTANT.....	41
C. HHC ACTUATION POWER REQUIREMENTS	41
VII. RESULTS.....	45
A. CONTROL SYSTEM FREEPLAY AND TORSIONAL CONSTANTS.....	45
1. Servo Actuator Assembly.....	45
2. Blade Pitch Link and Pitch Horn Assembly.....	46
3. Total System	48
4. Comparison of Individual Torsional Constant Data	49
B. BLADE FLAPPING HINGE TORSIONAL CONSTANT.....	51
C. HHC ACTUATION POWER REQUIREMENTS	51
VIII. CONCLUSIONS AND RECOMMENDATIONS.....	55
A. CONCLUSIONS.....	55
B. RECOMMENDATIONS	56
APPENDIX: MEMORANDUM OF UNDERSTANDING (Remotely Piloted Vehicle Operations at Fritzsche AAF).....	59
LIST OF REFERENCES.....	63
INITIAL DISTRIBUTION LIST.....	65

I. INTRODUCTION

The major characteristic that separates the helicopter from conventional fixed wing aircraft is its ability to hover. It derives this capability from the method by which it generates its lift. By utilizing rotating wings, or rotor blades, a helicopter is capable of generating the necessary aerodynamic forces to allow it to sustain vertical flight without translational velocity. The efficient accomplishment of vertical flight is, therefore, a fundamental characteristic of the helicopter rotor. But, with this ability to hover comes another fundamental characteristic of rotary winged flight, namely vibration.

Helicopter vibrations are detrimental in all respects. They are uncomfortable and fatiguing to the crew and passengers, they fatigue rotor and airframe components, and they damage delicate, costly components such as electronics. The reduction of airframe vibration constitutes a significant benefit with respect to enhanced safety, increased reliability, and reduced operating costs. Current vibration reduction technologies rely on passive devices which either isolate the source of vibration (isolators) or diffuse the vibration level (absorbers). The usefulness of these passive devices is normally limited to only a narrow range of flight conditions and vibratory frequencies. Also, the devices are heavy, requiring a reduction of the useful aircraft load. With helicopter design requirements focusing on wider mission capability, higher speeds, greater maneuverability and many possible configurations, an adaptive, weight effective vibration control system will have to be developed [Ref. 1].

To arrive at alternate means of vibration control, it is important to identify the major source of the vibrations. The primary causes of helicopter vibrations are the

rotor blade aerodynamic and inertial forces which are transmitted as excitation forces and moments from the rotor system to the airframe. Passive devices, as the name implies, attempt to reduce the effects of these vibrations after they have been generated. An active control concept, known as higher harmonic control (HHC), functions in a fundamentally different manner. By altering the aerodynamic loads on the rotor, vibratory forces and moments which cause the airframe to vibrate are reduced. This effectively reduces the prime source of the vibration excitation before it is produced and transmitted to the airframe.

Several methods of accomplishing HHC for different types of rotors have been considered. The most popular approach is blade feathering at the root using swashplate oscillations [Ref. 2]. Other forms of load variation include the use of jet flaps, servo-flaps, and circulation-controlled airfoils [Ref. 3]. The subject of HHC has been investigated by many researchers using numerical simulation, model testing in wind tunnels, and full scale flight testing. Full scale flight testing has demonstrated vibration reductions in the order of 25% to 90% [Ref. 4]. The wide range of variation in results from different tests shows two important points: (1) HHC is capable of reducing helicopter vibrations; and (2) further testing of actual HHC systems are warranted to fully understand their effects on the helicopter.

II. SCOPE

The Department of Aeronautics and Astronautics at the Naval Postgraduate School (NPS) is currently conducting research, at the master's and doctoral level, in the area of HHC. NPS research efforts, such as the work completed by LCDR Sarigul-Klijn on the application of Chaos methods to HHC [Ref. 5], have been supplemented with actual flight test data obtained from an OH-6A flight test program conducted by Hughes Helicopters, Inc. between 1982 and 1985. McDonnell Douglas Helicopter Company (MDHC), which acquired Hughes Helicopters, Inc. in 1984, has provided the flight test data which has proven to be invaluable for correlation with theoretical work. While the use of this archived flight test data is extremely helpful, it restricts the researcher to the study of phenomena which can be supported by this limited source of data. The ability to produce HHC data, specifically generated in support of a particular research goal, requires the institution of a helicopter flight test program. This appealing proposition is the basis for the work of this research effort.

Generation of flight test data requires a flight test vehicle specifically configured for the research initiative. Testing of an actual full-scale helicopter, while extremely attractive, was prohibited due to fiscal and operational constraints. Flight test experience, gained by the Department of Aeronautics and Astronautics Unmanned Air Vehicle (UAV) Flight Research Laboratory at NPS, demonstrated that quality flight test data was producible through the use of radio controlled aircraft. Expansion of the UAV program, to incorporate the testing of a Remotely Piloted Helicopter (RPH), was deemed the best method for generating HHC flight test data.

The decision to institute an RPH flight test program at NPS was made in April 1989. The goal of this research effort was the establishment of this program for the study of IHIC. From its inception, it was realized that the program would be an ongoing research effort that would span many students. Several intermediate stages were required to develop the program to a point where test flight data could be produced reliably. First, a determination of the attributes required of a RPH used for IHIC studies was required. Secondly, an RPH capable of completing the intended mission had to be found and acquired. Finally, modification of the RPH to an IHIC configuration was required. These stages correspond to the work pursued during this research effort.

III. BACKGROUND

As mentioned previously, HHC has been investigated by many researchers utilizing many different methods of research. Analytical studies, wind tunnel tests and flight tests have proven HHC capable of significant adaptive vibration reduction. [Ref. 1] While vibration reduction is the major emphasis of practically all HHC research, there are other variables which HHC affects. Hughes Helicopters' flight test results indicated a performance benefit from the use of HHC [Ref. 6:p. 18]. HHC also influences the loading of components such as rotor blades, pitch links, and associated dynamic components. The degree to which HHC affects these different variables is still unclear and in need of further testing.

A. PRINCIPLES OF HIGHER HARMONIC CONTROL

1. *The Origin of Helicopter Vibrations*

The energy sources supplying alternating forces to the helicopter are threefold: (1) air and inertial forces acting on the rotor; (2) engine and transmission vibrations; and (3) air forces acting on the fuselage, empennage, and other nonrotating parts of the machine. [Ref. 7] Of these alternating forces, rotor aerodynamic and inertial forces transmitted to the helicopter are the primary contributors. Airframe vibrations are directly related to the periodic forces and moments produced as the rotor blades revolve around the rotor hub. The forces acting at the blade root are the vertical shear force S_z and the in-plane shear forces S_x and S_y . The moments acting at the blade root are the flapwise root moment N_F and the lagwise moment N_L , which are small, or zero, for an articulated blade. The forces and moments occur periodically for each blade as it revolves about the hub.

Due to this periodicity, it is assumed that each blade experiences identical loading and motion. The forces and moments from each blade are transmitted through the rotor hub, which combines their effects and transmits the resultant forces to the airframe. The rotor hub acts as a filter between the rotating and nonrotating systems. N per rev vertical forces and moments, with N being the number of rotor blades in the rotor system, are transmitted from the rotating system to the nonrotating system at a frequency of N per rev. Rotating in-plane forces and moments at $N-1$ and $N+1$ per rev are transmitted to the nonrotating system at the frequency of N per rev. Therefore, the N per rev S_Z and N_L produce N per rev rotor thrust and torque, the $N-1$ and $N+1$ per rev S_X and S_Y produce drag and rotor side forces at N per rev, and the $N-1$ and $N+1$ per rev N_F produces pitch and roll moments at N per rev. This filtering simplifies the vibration problem since the rotor hub transmits only harmonics of the rotor forces and moments at multiples of N per rev. For real rotors, the N per rev harmonics dominate the vibration produced. [Ref. 8]

2. Higher Harmonic Control Inputs

HHC takes advantage of the rotor hub's ability to translate forces and moments from the rotating to the nonrotating system, and visa versa. By means of actuators, the helicopter's swashplate is excited in the collective, longitudinal cyclic, and lateral cyclic modes at N per rev, with resulting blade pitch oscillations at the three distinct frequencies of $N-1$, N , and $N+1$ per rev in the rotating frame. If these blade pitch oscillations are applied properly, they will generate a combination of unsteady aerodynamic and inertial loads to counteract the existing vibratory blade loads which cause airframe vibration. [Ref. 3]

Control of the HHC inputs can be broadly classified into two categories: open loop or closed loop. Open loop control refers to a system where the phase and amplitude of the HHC actuators are set manually with no feedback of airframe response. Closed loop control refers to a system which utilizes response feedback signals from onboard accelerometers, processes them with a suitable algorithm, and then adjusts the HHC actuators output to reduce the vibrations. HHC has been implemented successfully using various types of feedback controllers. Also, it has been found that the higher harmonic blade pitch inputs needed to suppress vibrations are small (typically less than two degrees), and therefore the power requirements for the actuators are manageable. [Ref. 2]

IV. RPH DEFINITION, ACQUISITION, AND SUPPORT

A. DEFINITION OF A SUITABLE RPH

To accomplish the intended goal of this research effort, it was important that the proper RPH was selected. A rotor system with three or more blades was required to fully study the effects HHC has on the force translations which occur at the rotor hub. Recent trends in helicopter design have shown a tendency toward utilizing four-bladed main rotor systems. This trend is seen by recent government programs which include helicopters such as the MDHC AH-64 (U.S. Army Apache), the Sikorsky UH-60A (U.S. Army Black Hawk) and SH-60B/SH-60F (U.S. Navy Seahawk/CV Helo), and the Aerospatiale HH-65A (U.S. Coast Guard Dolphin). Another example of the move to four-bladed rotor systems is the upcoming Bell AH-14BW SuperCobra designed for the U.S. Marine Corps. This program, which included replacing the aircraft's two bladed rotor system with the Bell 680 four-bladed, has demonstrated a 65% power increase [Ref. 9]. Due to this trend, a four-bladed RPH rotor system was chosen.

The gross weight of the RPH was the next consideration. The test platform had to be capable of supporting its own weight, the weight of the anticipated HHC actuation system, the weight of onboard data acquisition equipment, and still have sufficient power for basic flight performance. The weight of the HHC system was estimated at 10 pounds, which included four HHC actuators and their associated control equipment. Onboard data acquisition equipment was estimated at five pounds and encompassed the accelerometers (with conditioning units) and either an onboard data recorder or a telemetry transmitter. This equipment required the

RPH payload capability to be approximately 15 pounds. This payload requirement ruled out standard radio controlled model helicopters since their payloads are normally no greater than 10 pounds. Other considerations deemed necessary for an HHC RPH were: adjustable and readable rotor speed (Ω), a quality Pulse Code Modulation (PCM) radio control system, gyroscopic stabilization, and alternator equipped electrical system. One other constraint which had to be met was a total system cost no greater than \$10,000.

B. ACQUISITION OF THE RPH

With the general specification of the RPH formulated, a suitable aircraft had to be located. Local hobby stores were solicited for RPHs which met the requirements. This effort produced no results. Mr. Larry Jolly, helicopter columnist for *Model Aviation* (the official publication of the Academy of Model Aeronautics) was then contacted for recommendations. After reviewing his files, Mr. Jolly could recommend only one source which provided RPHs with the specifications needed. This was an RPH, produced by Pacific RPV of Startup, Washington, named the Bruiser. After receiving Bruiser specifications from Pacific RPV, the decision to proceed with procurement was made.

C. RPH SUPPORT REQUIREMENTS

I. Laboratory Facility

The NPS UAV laboratory, located in Bldg. 214, began fixed wing UAV research in 1987. The addition of an RPH to the existing UAV program forced the realization that the current laboratory space could not support both programs. Plans were instituted for the expansion of the laboratory from its current position

in Bldg. 214 to a larger room in the same building. Tools and associated maintenance materials may be shared by the UAV and RPH programs.

2. Flying sites

Under a memorandum of understanding between the Commander, Fritzsche Army Airfield (FAAF), Fort Ord, CA, and NPS, the runway facility at FAAF may be used for remotely piloted vehicle (RPV) operations. RPV operations at FAAF must be conducted with strict compliance to the memorandum of understanding, included as the Appendix, to insure continued availability of the runway. The runway facilities, which provide an excellent site to perform forward flight testing, is normally available only for weekend use. During the week, use is restricted by the normal operations at the field. Another site available for RPH testing is an actual helicopter pad located adjacent to the artillery range on Fort Ord Army Base. The asphalt pad, referred to as the Range 43 helo pad, is controlled by Fort Ord Range Control and its use is dependent on the operations being conducted in the area. The pad is suitable for hover testing but its use is limited for forward flight testing due to uneven terrain and trees in the area.

3. Piloting of the RPH

To operate the RPH safely and effectively, an experienced radio control helicopter pilot is necessary. NPS currently has no internal assets to pilot the RPH. Original intentions were to search the NPS local area for a radio controlled helicopter pilot that possessed the required skills to fly the RPH. It was also required that the pilot had an interest in the associated research effort since no remuneration was available. This plan was not successful. The UAV laboratory is expected to hire a UAV technician who is a capable fixed wing RPV pilot. The current plan is to train the technician to pilot the RPH. While the training is

expected to be a long term process, the department will have an internal asset capable of piloting the RPH for flight tests.

V. THE REMOTELY PILOTED HELICOPTER SYSTEM

A. AIRCRAFT DESCRIPTION

The RPH chosen for this project, shown in Figures 1, 2, and 3, was designed and built by Pacific RPV, a company based in Startup, Washington. The RPH, named the Bruiser by Pacific RPV, was originally designed to provide a platform for still and video cameras, spray equipment, tethered instruments, and electromagnetic countermeasures (ECM). The RPH, available with either a two or four-bladed rotor head, was procured with the four-bladed head.

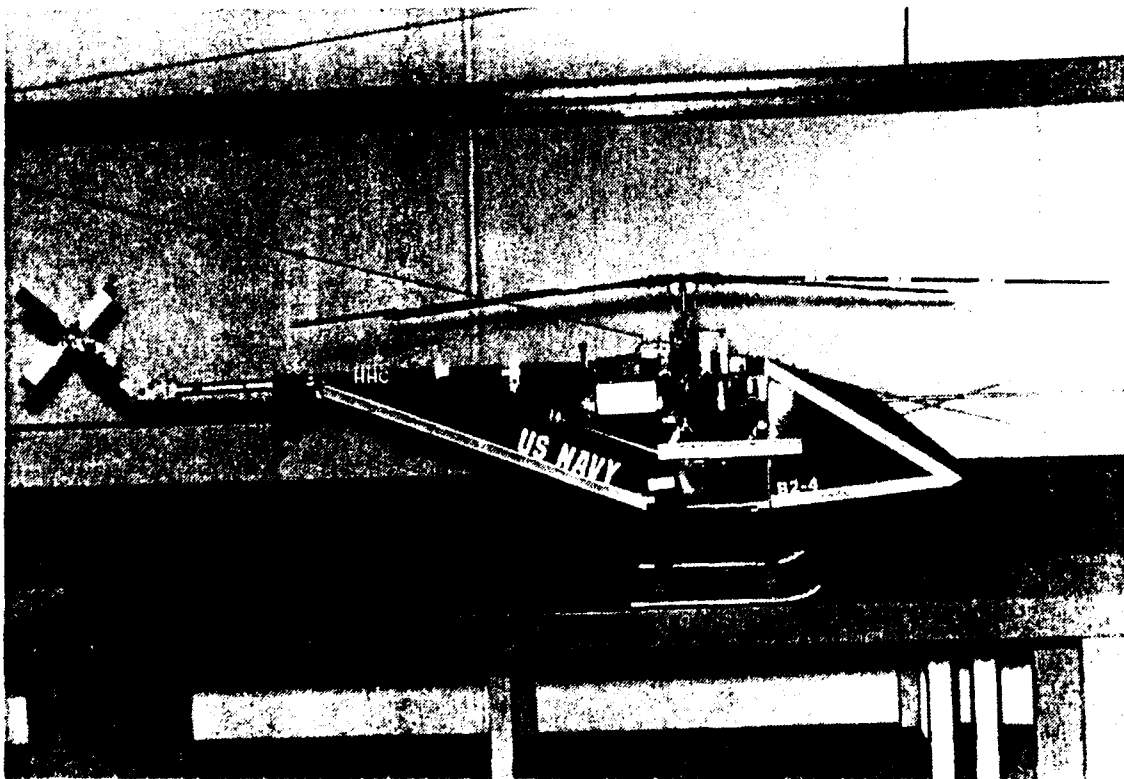


Figure 1. The Remotely Piloted Helicopter (Side View)

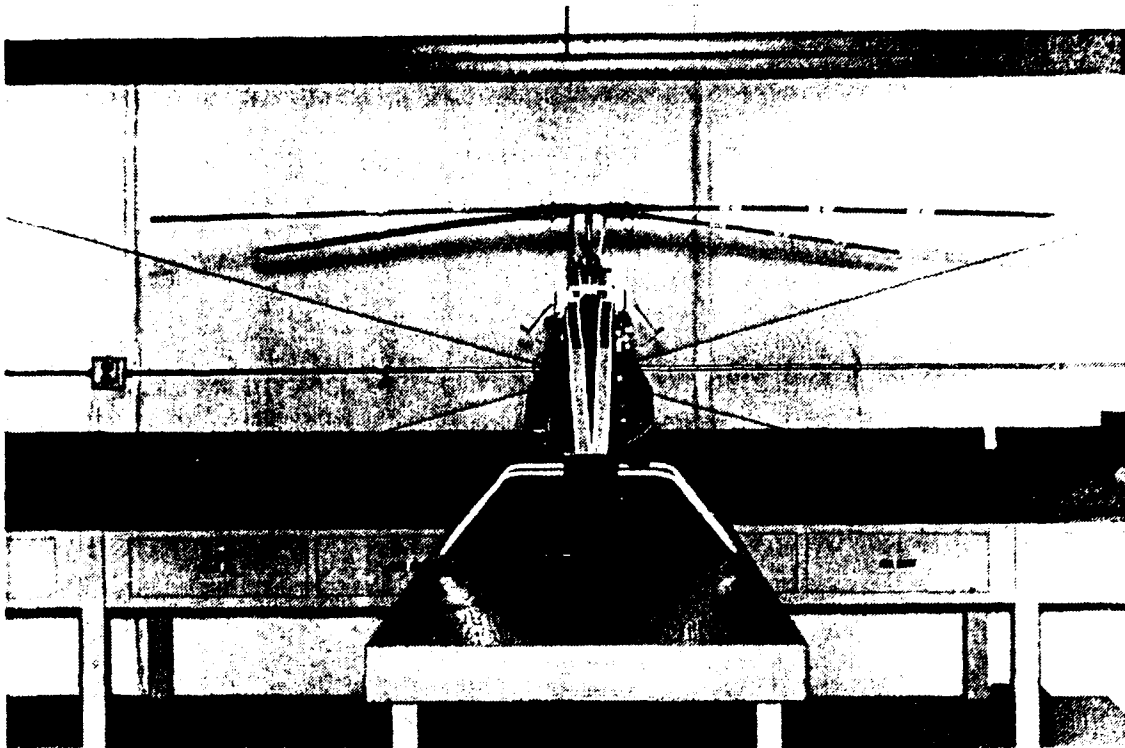


Figure 2. The Remotely Piloted Helicopter (Front View)



Figure 3. The Remotely Piloted Helicopter

1. Airframe

The RPH's main airframe is constructed of aircraft grade 7075-T6 acid etched aluminum which has been painted with an anti-corrosion epoxy coating. The forward portion of the fuselage consists of a nylon support shelf which is covered by a lexan fairing. Figure 4 shows the forward portion of the fuselage with the fairing removed. Two aluminum blocks are mounted on the support shelf.

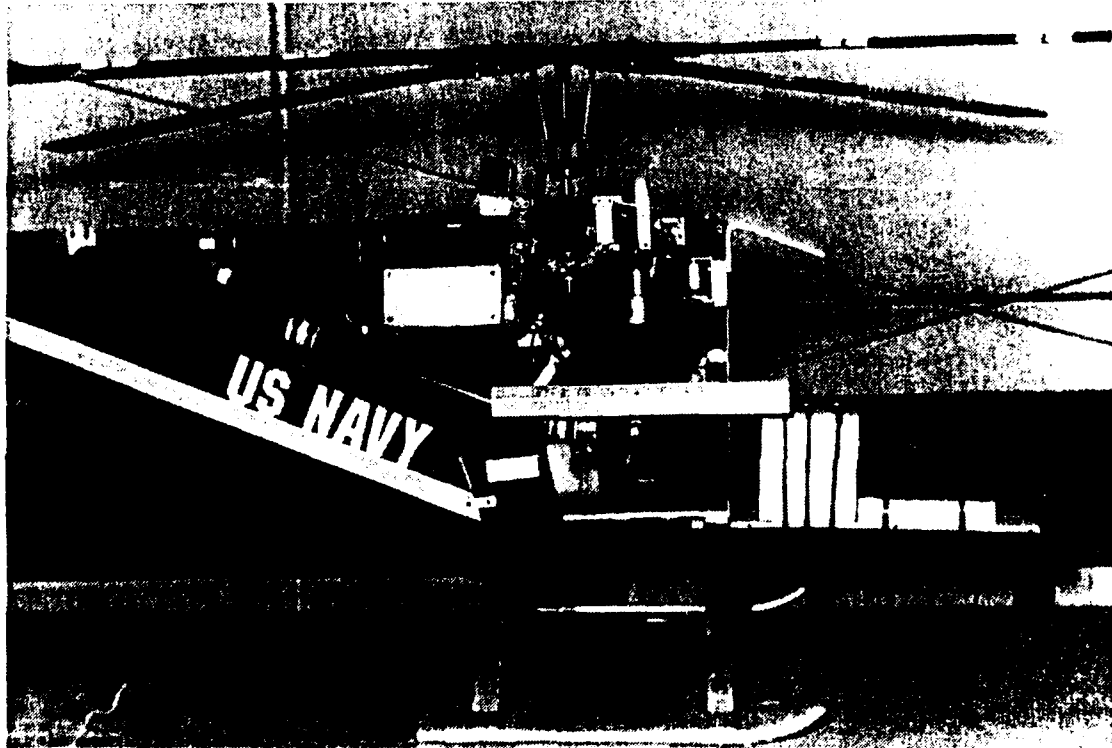


Figure 4. Fuselage with Fairing Removed

These blocks, weighing approximately five pounds, balance the longitudinal center of gravity for the no payload configuration. Cargo payloads may be mounted to the support shelf or the shelf may be removed to facilitate special mounting requirements of the payload. The tail boom is an aluminum tube with an aluminum horizontal stabilizer. The horizontal stabilizer increases longitudinal stability in

forward flight and provides a convenient mounting point for the flight control receiver and tele-tachometer/airspeed indicator transmitter antennas. A lexan fairing is installed on the aft section of the fuselage along the tail rotor boom support rods. This fairing is a cosmetic addition and is not required for flight. The landing gear consists of aluminum struts and skid tubes.

2. Rotor System

a. Rotor Head

The RPH is equipped with a four-bladed, fully articulated rotor head. Figure 5 shows the rotor head installed on the RPH and Figure 6 is an exploded view showing the associated internal components. Each rotor blade's flapping axis is defined by a horizontal bolt which passes through the axle housing and blade grip

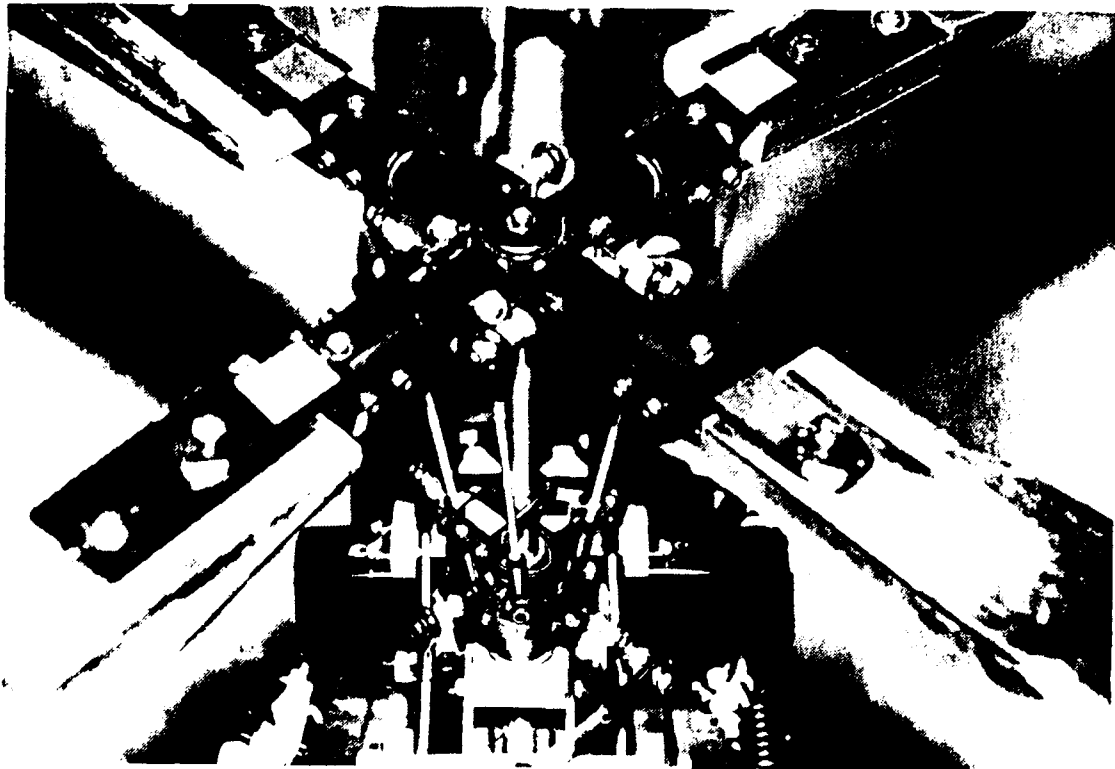


Figure 5. RPH Rotor Head

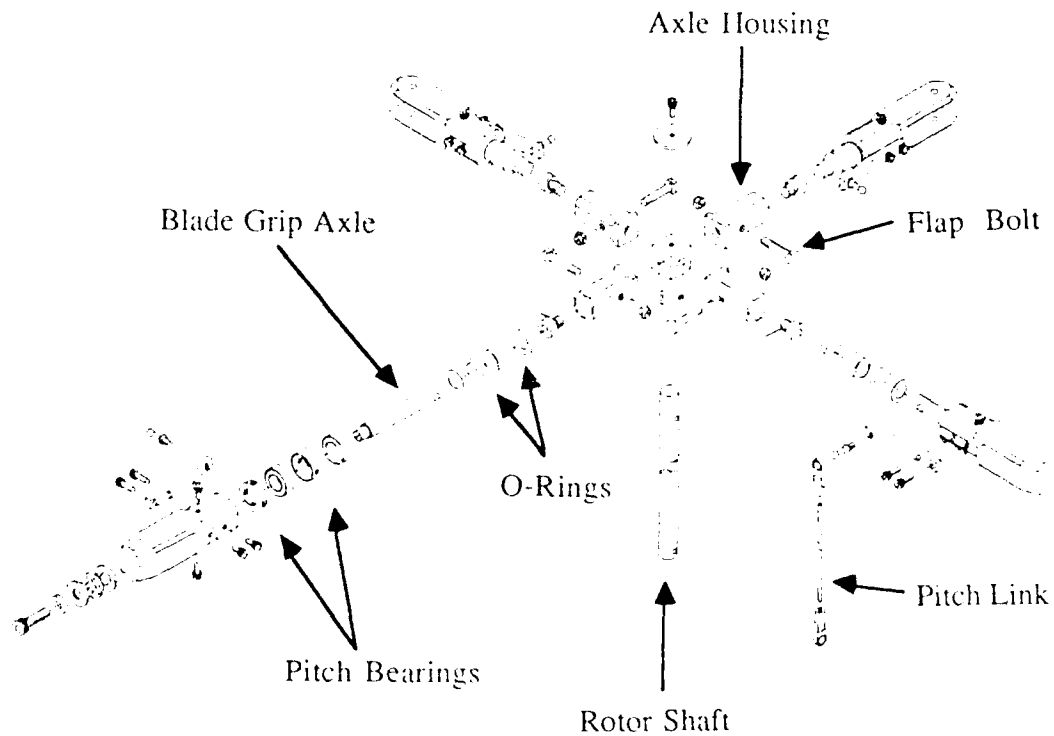


Figure 6. RPH Rotor Head (Exploded View)

axle. The blade pitch axis is coincident with this axle. The rotor blade lead-lag axis is defined by the blade retaining bolt which passes through the blade grip. Flap damping is provided by two rubber o-rings which are installed on the blade grip axle. Damping is achieved by the compression of the o-rings inside the axle housing as the blade flaps. The maximum flapping angle, defined by the geometry of the axle and axle housing, is approximately $\pm 5^\circ$. Lead-lag damping is provided by friction between the blade and the blade grip and is controlled by the torque applied to the blade retaining bolt. The rotor head is attached to the main rotor shaft which is made from 4130 steel.

b. Rotor Blades

The rotor blades are a maple/balsa wood combination, impregnated with polyester resin. Each blade weighs approximately 280 grams and has a lead

weight imbedded in the outboard leading section to adjust the center of gravity to approximately the quarter chord position. A NACA 2415 airfoil section is utilized and no blade twist is incorporated. Stainless steel bearing plates are mounted to the blade roots to transfer blade stresses to the rotor hub's blade grips. The plates are attached to the blade root with epoxy and a bolt. Table 1 presents the characteristic of the main rotor system.

TABLE 1. ROTOR SYSTEM CHARACTERISTICS

Number of Blades	4
Blade Length:	37.6 in (3.13 ft)
Blade Weight:	9.88 oz.
Rotor Radius:	39.7 in (3.31 ft)
Disc Area :	4,951.4 in ² (34.38 ft ²)
Flapping Hinge Offset:	0.75 in (0.0625 ft)
Chord:	2.1 in (0.175 ft)
Blade Area:	333.48 in ² (2.315 ft ²)
Solidity:	0.06735
Tip Speed ($\Omega = 1,100$ RPM):	4,573.1 in/sec (381.09 ft/sec)

3. Flight Control System

The flight control system employed by the RPH is capable of generating the required pitch, roll, collective, and yaw responses for safe flight performance. Pitch, roll, and collective flight control is achieved using a swashplate arrangement to change rotor blade cyclic and collective pitch. The swashplate and associated control components are seen in Figure 7. Flight control rods, used to transfer

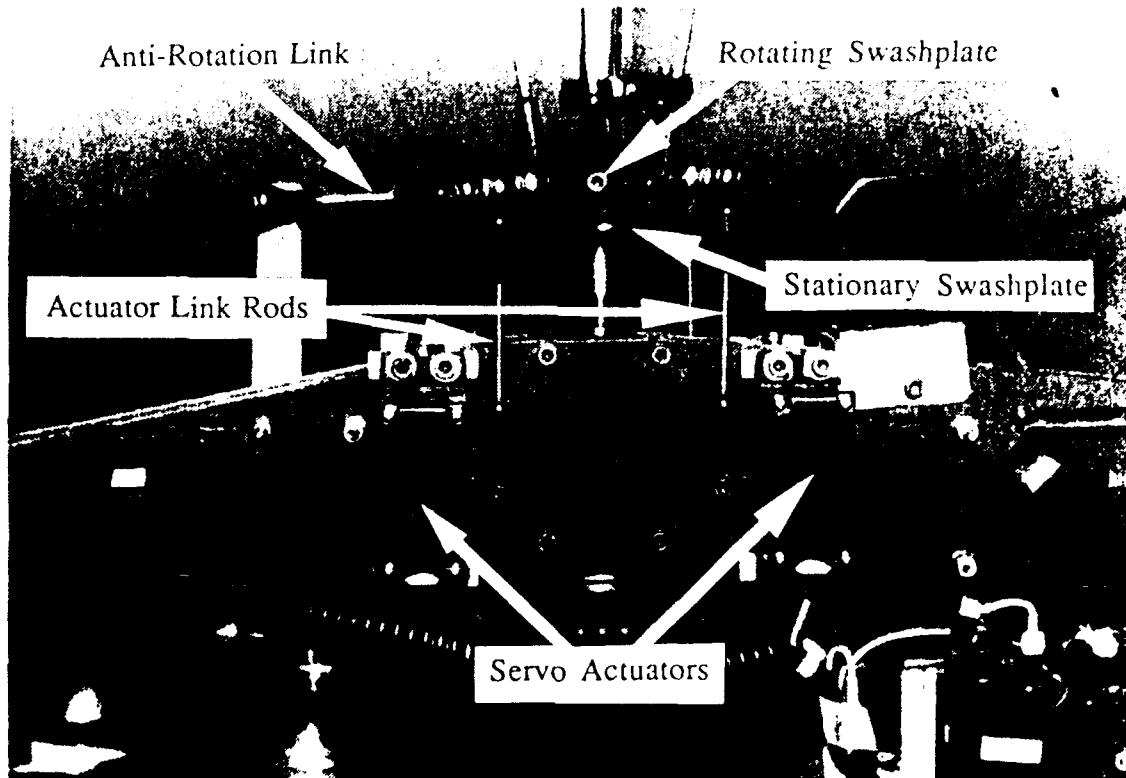


Figure 7. Swashplate and Associated Control Components

linear motions in the flight controls, are made of stainless steel. The control rods are threaded at each end to facilitate the plastic ball end links. This threaded arrangement allows for adjustment of the link lengths, an important feature when adjustments for blade track or flight control mixing is desired. The ball end links snap onto 1/4 inch ball ends which serve as the component's link attachment point. Four electric servos, connected to the stationary swashplate by the actuator link rods, operate in unison to generate the necessary control response. The actuator link rods are attached to the stationary swashplate at four ball ends which are 90° apart. The anti-rotation link, seen in Figure 7, prevents the stationary swashplate from rotating and maintains it in the correct orientation with respect to gyroscopic

precession. The rotating swashplate also has four ball ends which are connected to the blade grip pitch horn ball ends by pitch links. Four servos function in pairs to generate pitch and roll inputs to the stationary swashplate. To illustrate the method in which flight control is achieved, the effects of a right roll input will be explained. Figure 8 shows a schematic of this process with respect to both the rotating and nonrotating portion of the flight controls. When a right roll input is commanded, the right forward roll servo pulls down on its ball end while the left aft roll servo pushes up on its ball end an equal amount. The forward left and aft right pitch servos do not move and their ball ends define the axis about which the swashplate rotates. The roll servos' outputs, therefore, cause the stationary swashplate to pivot about this axis, the swashplate roll axis. The rotating swashplate, which rotates in a plane that is parallel to the stationary swashplate, transmits the control response to the individual blade pitch horn ball ends. The pitch horn ball ends lead the blade pitch axis by approximately 45° . The individual rotor blades then cyclically decrease angle of attack in the forward section of the rotor disk while cyclically increasing the pitch an equal amount in the aft section of the rotor disk. Gyroscopic precession delays the response of the blade pitch action approximately 90° . The net effect of the control movements is the generation of a right rolling moment on the helicopter.

Pitch control is achieved in a similar manner, with the pitch servos moving while the roll servos maintain their position. Collective control is achieved by all four servos either raising or lowering the entire stationary swashplate in unison. This action causes all the rotor blades to increase or decrease blade angle of attack by equal amounts. Helicopter yaw control is provided by a separate servo

which collectively increases or decreases the four-bladed tail rotor's pitch. The tail rotor assembly is shown in Figure 9.

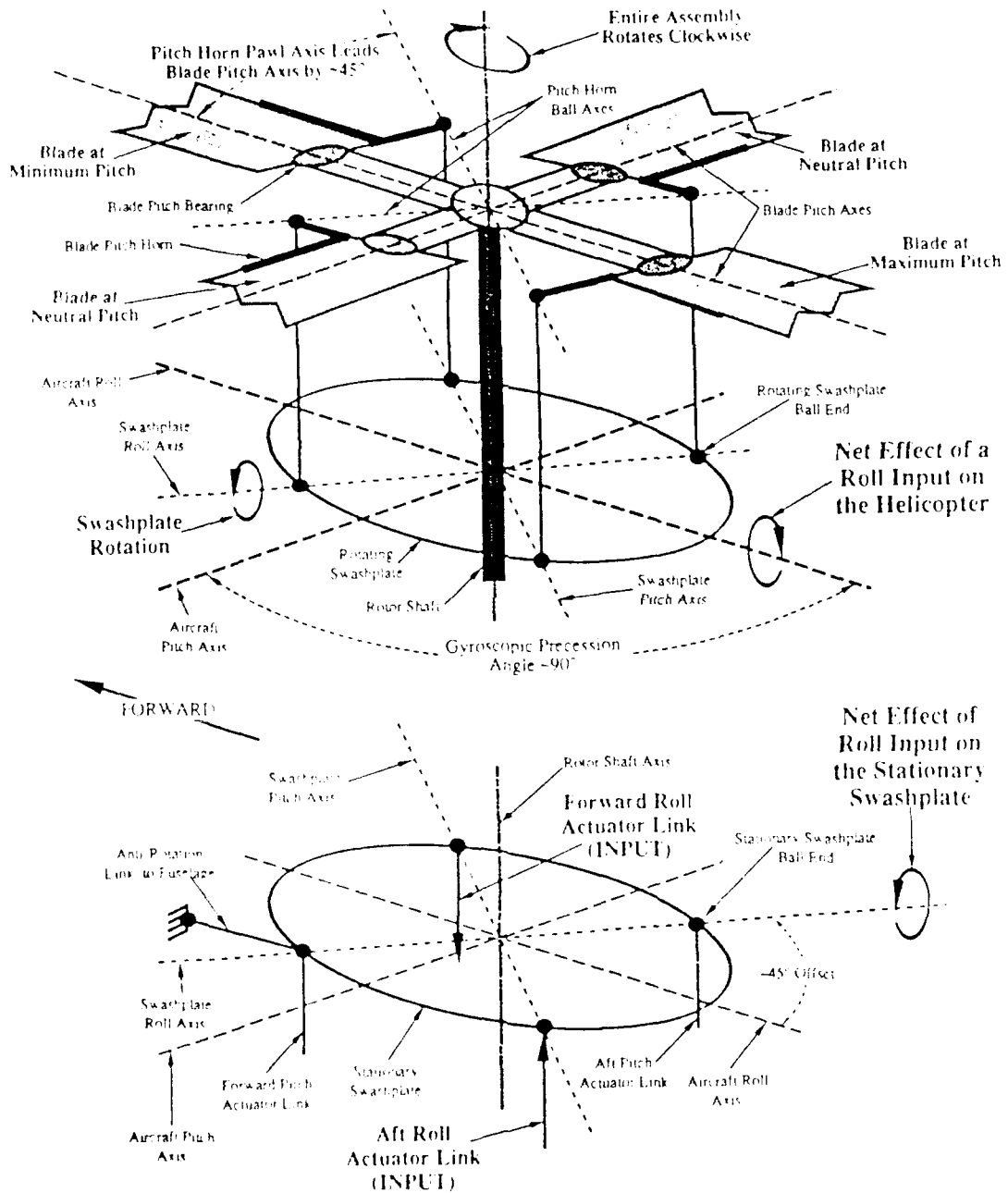


Figure 8. Schematic Representation of a Roll Control Input on the Stationary and Rotating Swashplates



Figure 9. Tail Rotor Assembly

4. Radio System

The RPH is controlled by a Futaba® radio system consisting of a nine channel, programmable FP-9VHP transmitter, the FP-R129DP receiver, five FP-S9201 servos, five FP-G154 rate gyros, and a 1,000 milliamp-hour (Mah) rechargeable nickel cadmium (NiCd) battery.

a. Transmitter

The transmitter, seen in Figure 10, utilizes pulse code modulation (PCM) for radio signal transmission. PCM digitally encodes the transmission signals to reduce interference and optimize servo resolution and response. The transmitter is capable of storing the control attributes for up to six separate RPHs.

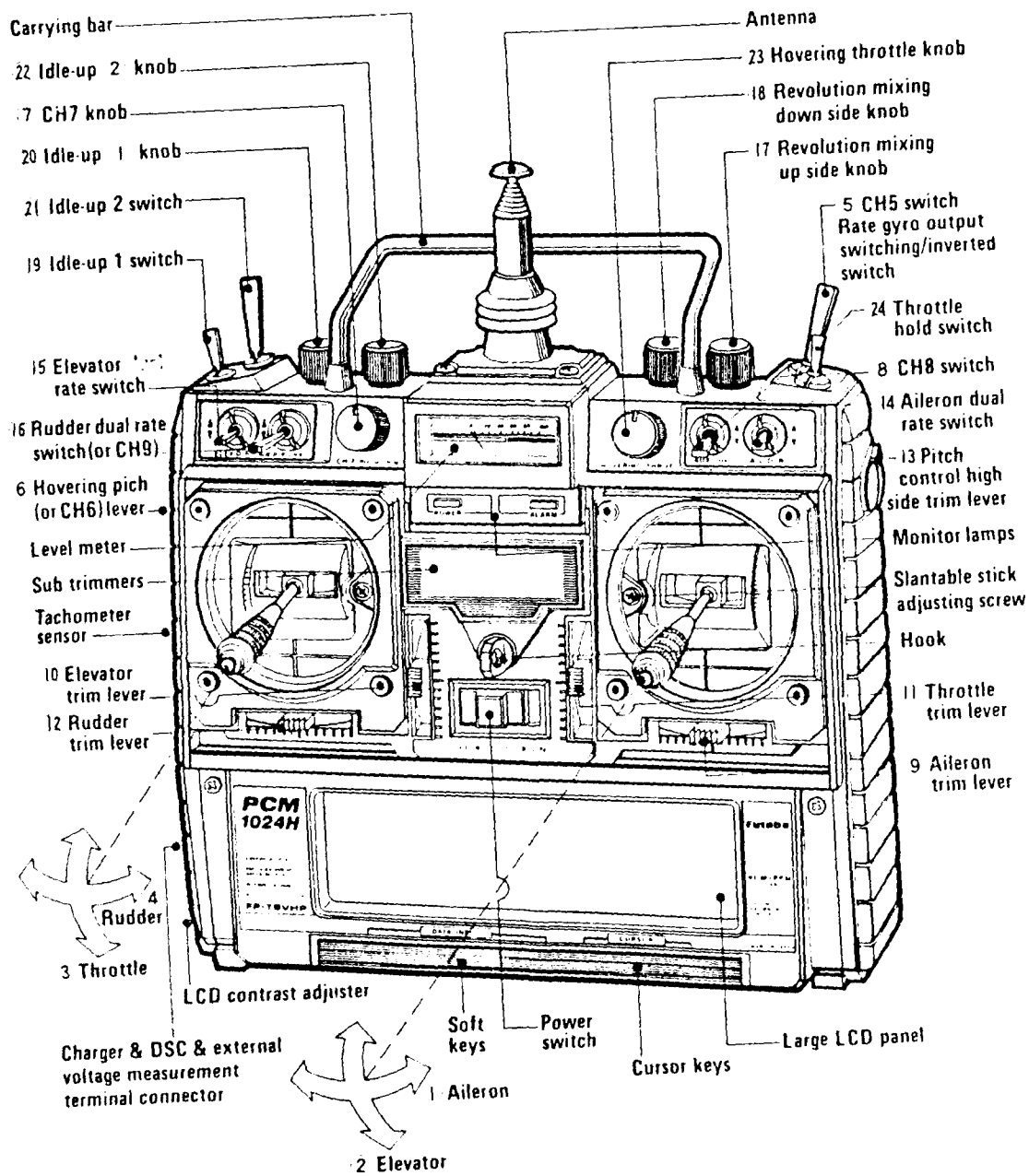


Figure 10. Radio Control System Transmitter

Stored program data can be displayed on a Liquid Crystal Display (LCD). Programming and cursor keys, accessible under a protective cover below the LCD screen, are used for data entry or adjustment. The transmitter is powered by an internal 9.6 volt NiCd battery. When fully charged, the battery can provide approximately 100 minutes of transmitter operation. A low battery warning is incorporated to ensure the RPH is not jeopardized by a low transmitter battery voltage condition. When battery voltage drops below 8.5 volts, the message "LOW BATTERY" blinks on the LCD display and a buzzer sounds. This allows the RPH to be safely landed before radio transmission is interrupted by the low battery state.

b. Receiver

The receiver amplifies the received signal and then processes it using a PCM decoder. This decoder separates the main transmission signal into nine individual channels of information and routes each channel to its respective servo. While nine channels are provided, only six are utilized for the control of this RPH. These six channels are allocated for specific flight control functions as shown in Table 2. To provide some protection against interruptions in the received signal, a hold and fail safe system is provided. If a loss of signal occurs, the hold function maintains the servos in the position held just before the normal signal was lost. If the interruption lasts longer than one second, the receiver sends all servos to a pre-set, or fail-safe position. When a normal signal resumes, fail-safe is released. The fail-safe position is programmed into the transmitter prior to flight and is consistent with the control inputs required for normal, straight and level flight. The fail-safe data is automatically sent to the receiver when the transmitter is turned on and at one minute intervals as long as the transmitter is on. This

protection is not intended to act as an autopilot and will only be useful for short periods of signal interruption.

TABLE 2. RECEIVER CHANNEL ALLOCATION

Channel	Controls Response of
1	Right Forward Roll Servo
2	Right Aft Pitch Servo
3	Unused
4	Tail Rotor (Yaw) Servo
5	Unused
6	Left Aft Roll Servo
7	Throttle Servo/Engine RPM governor
8	Left Forward Pitch Servo
9	Unused

The receiver also protects against a low aircraft battery condition. By constantly monitoring the battery voltage, the receiver immediately recognizes a low battery condition. When this occurs, the receiver moves the throttle servo to a pre-set position, normally set at slightly above idle. This is immediately recognized by the pilot, since the RPII's power setting will be lower than normal. When this happens, the pilot can release the battery fail-safe throttle position cycling the throttle stick or by moving the channel nine switch to the up position. This regains normal control and allows the pilot approximately 30 seconds to make a safe landing. After the 30 seconds, the receiver may stop functioning due to the lower battery condition.

c. Servo Actuators

Flight control movements and throttle control are accomplished by six FP-S9201 servos. Each servo uses an electric motor to drive a splined output shaft to which a splined plastic actuator output arm is attached. The servo maintains the correct position by monitoring its output position and the position signal from the receiver. When a difference in the two signals exists, an error signal is generated. The servo motor then moves the output shaft in the direction which cancels the error signal. The output shaft rotates a minimum of $\pm 45^\circ$ from its neutral position and has a speed of approximately $270^\circ/\text{sec}$. At a weight of 1.8 oz., the servo is capable of generating a continuous output torque of 69.5 oz.-in. The servo actuators, while capable of providing the control displacements necessary for normal flight, are incapable of producing the necessary oscillatory frequencies required for HHC implementation.

d. Gyroscopic Stabilization

Rate stabilization is utilized for the pitch, roll, and yaw axes to reduce pilot workload and provide a more stable platform for data acquisition. The gyroscopic stabilization inputs are introduced between the receiver and the individual servos. Therefore, two gyros are necessitated for both the pitch and roll axes, while only one is required for yaw stabilization. The gyros are seen in Figure 11. Pitch and roll gyros may be turned off to conserve battery power when the aircraft receiver is operated during radio adjustment or preflight checks. Because the helicopter is neutrally stable in pitch and roll, it is extremely important that these gyros be turned on prior to flight. The yaw gyro cannot be deselected because its stabilization is critical to the safe operation of the RPH. [Ref. 10]

5. Electrical System

The RPH onboard electrical system consists of a 1,000 Mah NiCd battery and a brushless alternator. The electrical system provides power to the radio receiver, flight control servos, RPM governor, and the tele-tachometer/airspeed indicator system. A rubber belt, which runs on a pulley mounted to the RPH's engine shaft, turns the brushless alternator. The alternator, seen in Figures 11 and 12, provides an output of approximately 5.3 volts. It supplies three watts of

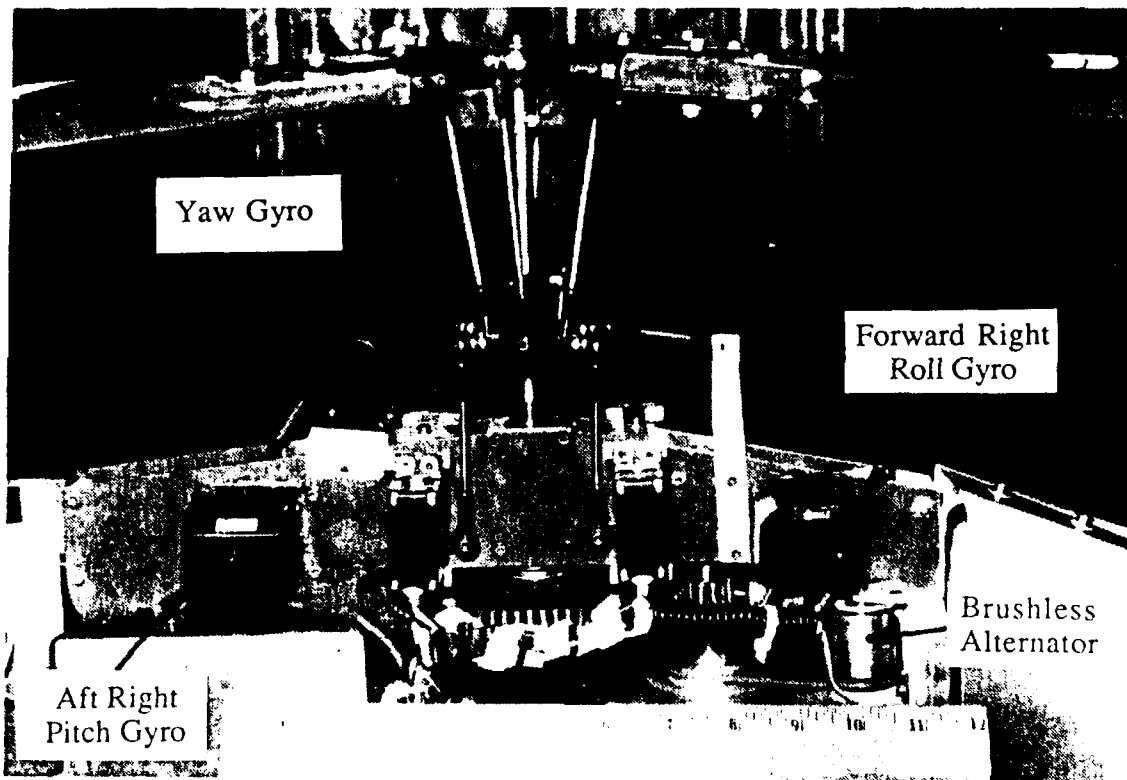


Figure 11. Flight Control Gyros

continuous power and a peak rating of five watts. The power requirements of the electrical system, when all components are operating, is approximately 3 watts. It is extremely important that the battery pack be fully charged prior to flight. This

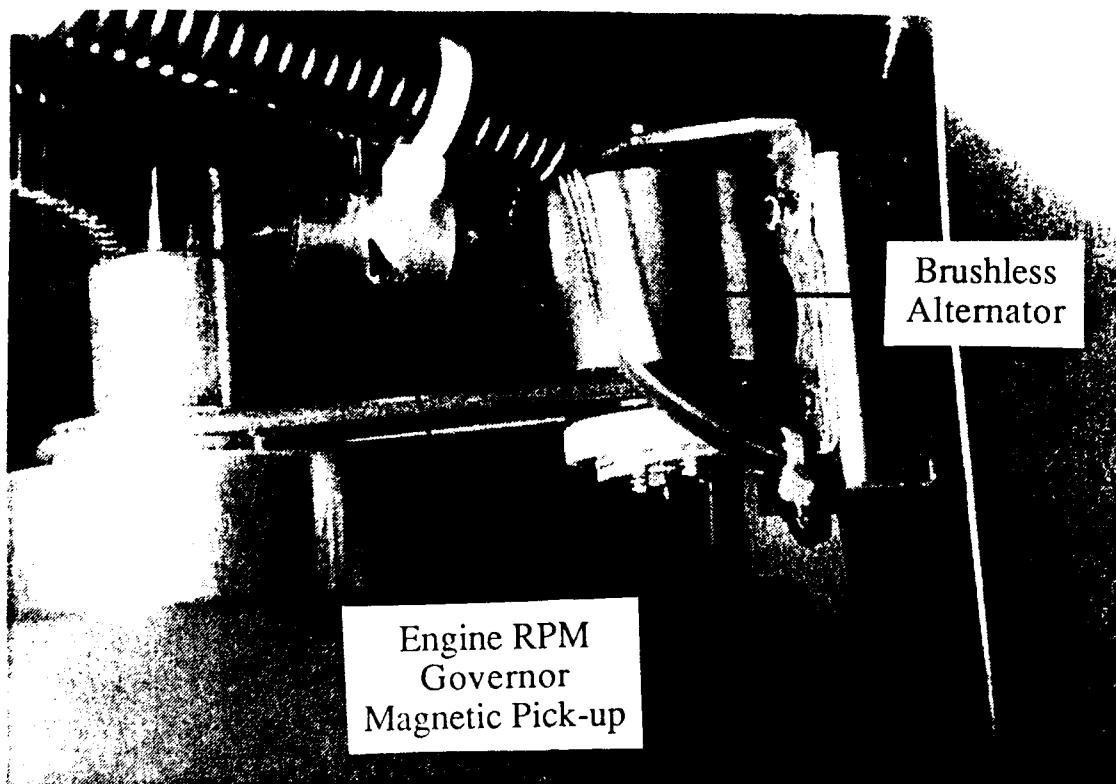


Figure 12. Brushless Alternator

is mandated because prior to engine start, the battery provides all required electrical power. Also, the alternator output is not sufficient to provide a charging current to the NiCd battery.

6. Powerplant

a. Engine

The helicopter is power by the two cylinder, two cycle, air cooled T77i Super Tartan® engine seen in Figure 13. Engine displacement is 2.669 cubic inches with a compression ratio of 9.5 to 1.0. The engine is equipped with an electronic ignition system, and is started with a recoil pull starter. The output of the engine, as installed with tuned mufflers, is approximately four B.H.P. at 8,800 R.P.M. Maximum torque from the engine is 30.35 in. lb. at 7,000 R.P.M. The

Installed in RPH
Without
Propeller Spinner

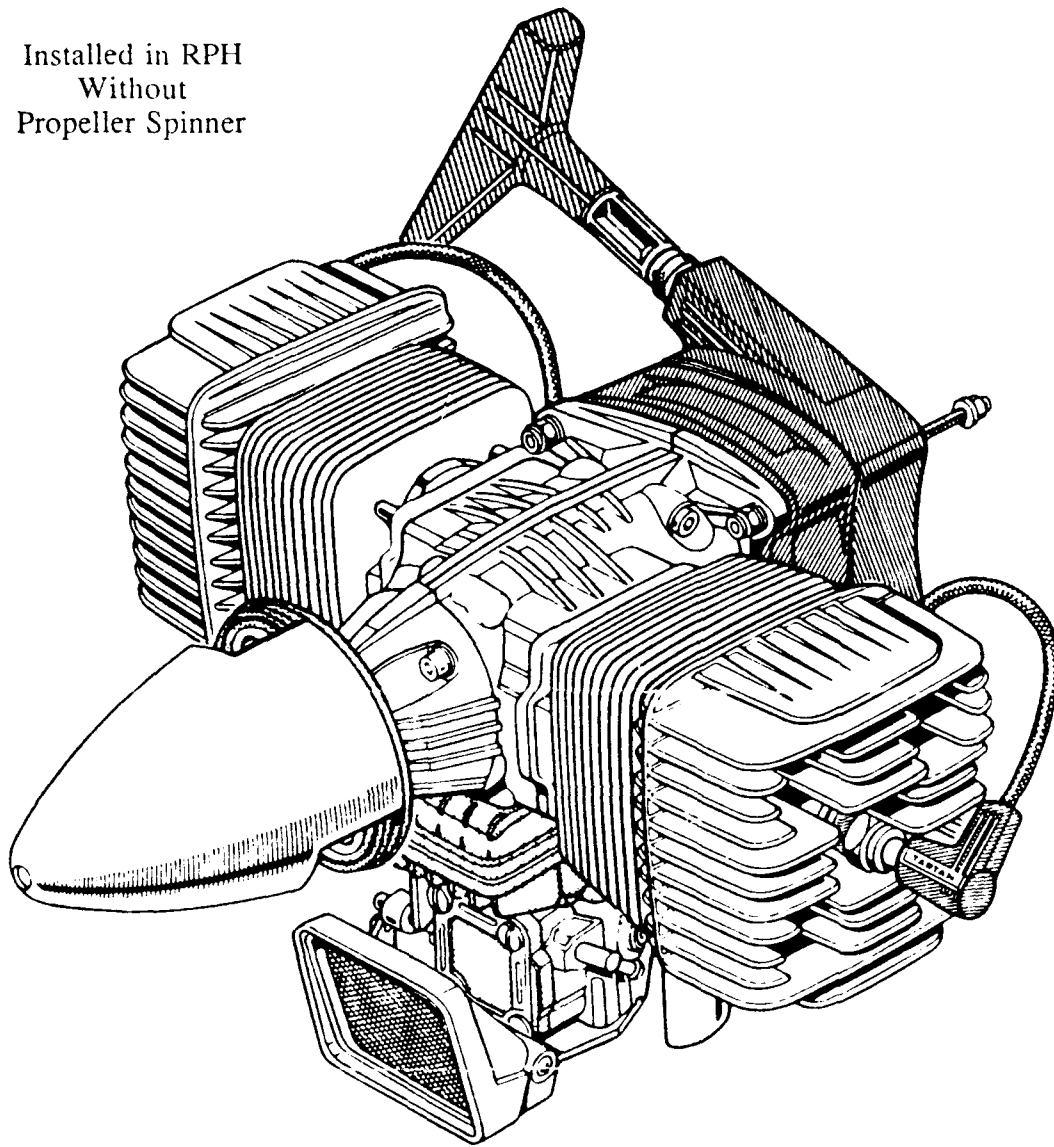


Figure 13. T77i Super Tartan® Engine

engine weighs approximately 5.5 pounds and runs on a 5% oil/95% gasoline (98-100 octane) mixture. Fuel tank capacity is 24 oz. with the air-to-fuel mixture being controlled by the all position diaphragm carburetor and fuel pump. Ignition spark is achieved using a 10X1 mm spark plug.

b. Drive System

The engine drives the main drive gear assembly which is located on the lower end of the rotor shaft and is visible in Figure 11. A one-way sprag clutch is installed in the center of the main drive gear to allow for autorotative flight. The associated gearing ratio of 6.56 dictates an engine speed of 7,216 RPM for the normal operating rotor speed of 1,100 RPM. Tail rotor drive is achieved by a fiberglass belt drive which runs, via pulleys, from the main rotor drive shaft through the tail boom tube, to the tail rotor drive shaft. Figure 14 shows the tail rotor drive belt at the tail rotor drive shaft pulley.

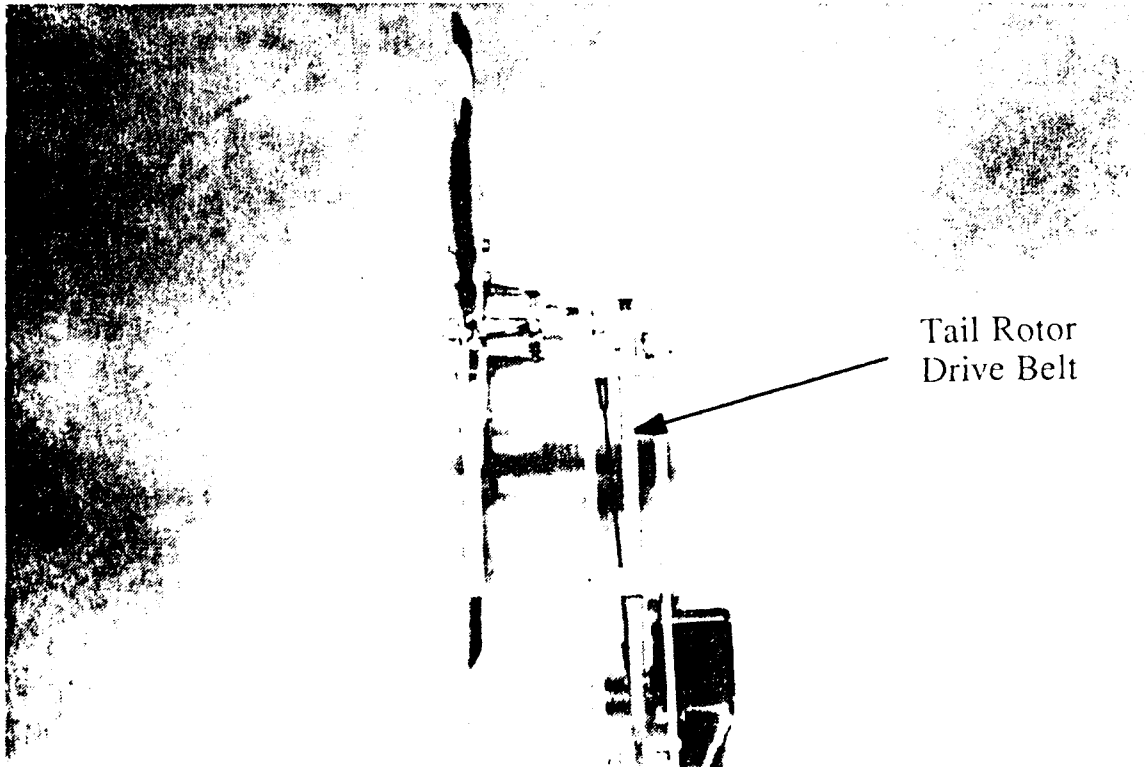


Figure 14. Tail Rotor Drive Belt at the Tail Rotor

c. Engine RPM Governor

Control of engine RPM is achieved electrically using an RPM governor system. Engine RPM is sensed by a magnetic pick-up from the steel gear which drives the main drive gear. This magnetic pick-up is visible in Figure 12. The signal from the magnetic pick-up is converted into a pulse frequency which is proportional to rotor RPM. The RPM governor is set to a specific pulse frequency which correlates to the desired engine RPM. When a difference in the compared signals is sensed by the governor, it changes its output pulse frequency to the throttle servo, which returns the engine to the desired RPM. A schematic of the system is shown in Figure 15. The channel seven rotary control knob (see Figure 10) on the transmitter is used to control the desired engine RPM. The RPM governor operates between a pulse frequency of 1,000 and 4,000. Therefore, the lowest possible rotor speed that can be controlled is approximately 720 RPM which is unacceptable for engine start and shutdown. To safely accomplish engine start

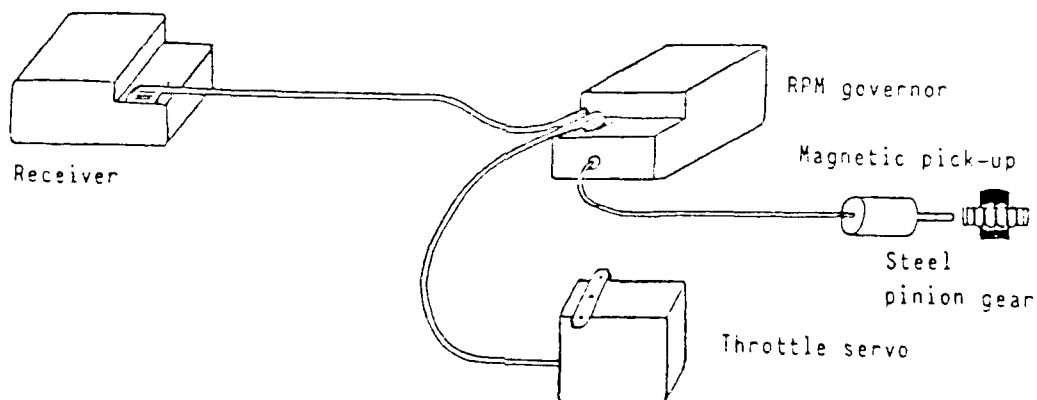


Figure 15. Engine RPM Governor System

and shutdown, the governor is deactivated during the first 1/2 of the control knob's rotation. The first quarter of control knob rotation is set to the idle region for the throttle servo. The second quarter of control knob rotation is a deadband region, in which the throttle servo does not respond. When the control knob is advanced passed this deadband range, the throttle servo is slowly advanced to the full power position, and governing is provided. The final rotor speed is then a function of the control knob's position in the last half of its rotation.

7. Telemetry Equipment

The Digicon© TT-01 Tele-Tachometer/Airspeed Indicator System provides rotor speed and airspeed information for the helicopter. The system consists of a hand held receiver/monitor, an airborne transmitter, two electro-optical sensors, and a low and high speed sensor. The system utilizes electro-optical sensors which measure the frequency at which light to the sensor is interrupted. Figure 16 shows the main rotor sensor with its associated sun shield.

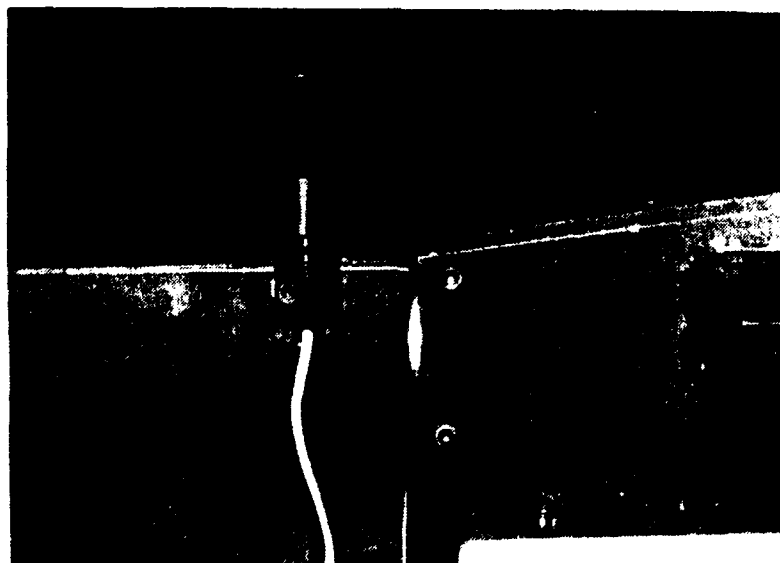


Figure 16. Main Rotor RPM Sensor

The sensor, mounted approximately ten inches aft of the main rotor shaft, detects the frequency of blade passage and the airborne transmitter sends the corresponding signal to the receiver/monitor, seen in Figure 17. The received



Figure 17. Tele-Tachometer/Airspeed Indicator Receiver/Monitor

signal is divided by four and this value is displayed on a needle indicator when the function switch is set to "rpm" and the appropriate scale is chosen. Airspeed information is derived from a low speed sensor mounted under the RPH's fuselage. This airspeed sensor, seen in Figure 18, is a calibrated propeller, mounted in front

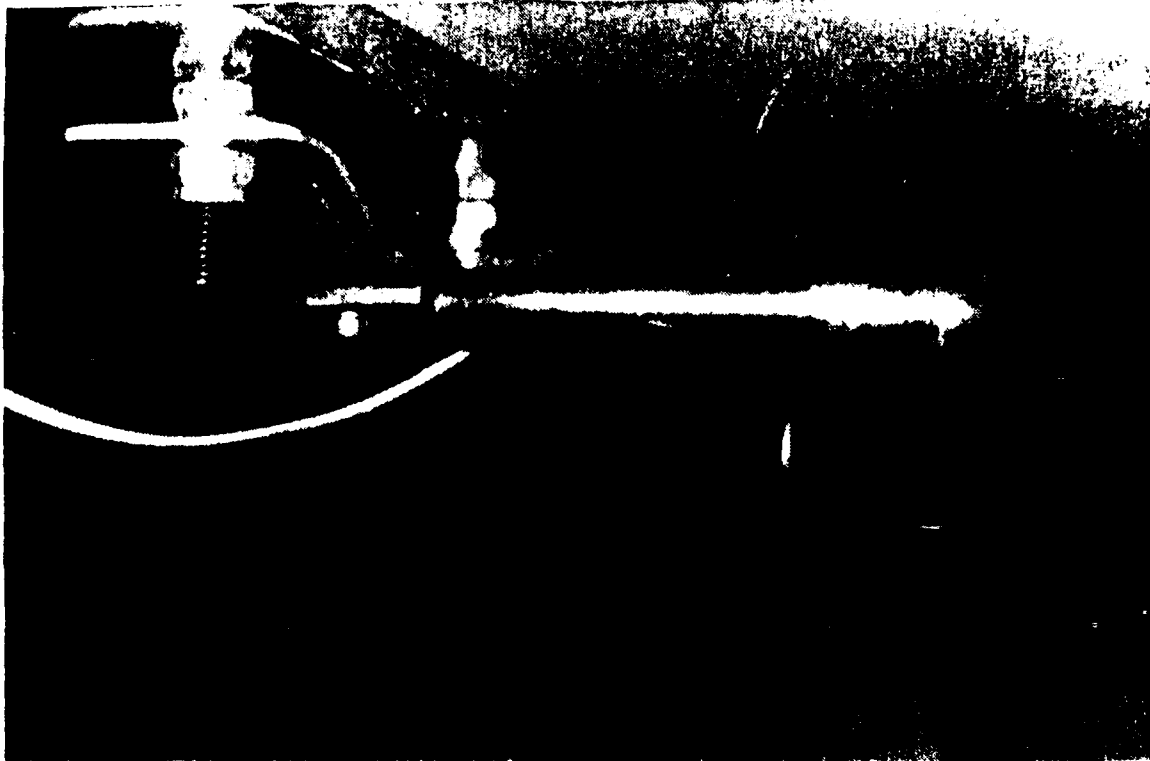


Figure 18. Airspeed Sensor

of an electro-optical sensor. As the propellor is turned by the airflow under the fuselage, its blades interrupt the light to the sensor. This generates a proportional airspeed signal which is transmitted to the receiver/monitor. Airspeed information, in kilometers per hour, is displayed on the needle indicator when the function switch is set to "km/hr."

VI. HIGHER HARMONIC CONTROL MODIFICATIONS

With the RPH acquired, modification of the control system to incorporate HHC actuation was necessary. Before any modifications could be accomplished, a knowledge of certain control system parameters was required. Of initial interest were the control system components' freeplays and spring constant values. These values were very important since they affect the transmission of displacements from the servo actuators to the rotor head.

Hughes Helicopters, Inc. realized the importance of the freeplay and spring constant values in 1981 when a complete review of the OH-6A's control system was necessitated by poor HHC system response. The original attempt at employing HHC on the OH-6A was hampered by excessive freeplay and relatively low stiffness values for the control system. The original system had an effective worst case freeplay of ± 40 mils and an effective spring constant of 2,000 lb./in. These values severely reduced the transmission of control motion from the actuators to the blades. To remedy the situation, Hughes elected to redesign the systems' components. System freeplay was reduced by replacing rod-end bearings, ball bearings, bolts, and the swashplate assembly with carefully selected, high tolerance components. System spring constants were increased by replacing the magnesium components with materials which had a higher Young's Modulus. The stationary swashplate and the longitudinal bellcrank and idler were remanufactured from aluminum and the lateral bellcrank and collective mixer bellcrank were remanufactured from 4310 steel. These material substitutions increased the components spring constants by reducing the strain associated with loading. The net effect of the redesign yielded a worst case freeplay of ± 10 mils and an effective

spring constant of 5,000 lb./in. These values proved to be acceptable for the successful implementation of HHIC on the OH-6A. [Ref. 11]

To determine the freeplay and spring constant values for the RPH, a method of testing these values was required. To provide uniformity in the RPH measurements, all spring constants for the control system were referenced to rotor blade pitch angles. Therefore, instead of linear spring constants, rotational torsional constants were necessitated. The torsional constant of the blade flapping hinge was also determined for full definition of the rotor head components' attributes. Another important value to determine was the power required to drive the rotor blades at the higher harmonic frequency.

A. CONTROL SYSTEM FREEPLAY AND TORSIONAL CONSTANTS

The control system components which required analysis were the servo actuators and linkages, the swashplate assembly, and the blade pitch link and pitch horn assembly. By treating the control system as a system of springs and freeplays, as shown in Figure 19, the characteristics of the components could be analyzed. A methodology for experimentally determining the freeplay and torsional constants for these systems parameters was devised. By loading the component with a known force and recording the associated deflection, the torsional constant was calculated graphically by computing the slope of a line through the points. Freeplay was also determined with this graphical method by noting the offset of the x-axis intercept from zero. The swashplate assembly was the only component which could not be isolated for loading. To calculate this torsional constant, an assumption that all torsional constants were linear was required. This assumption facilitated the superposition of torsional constants to compute the unknown swashplate value.

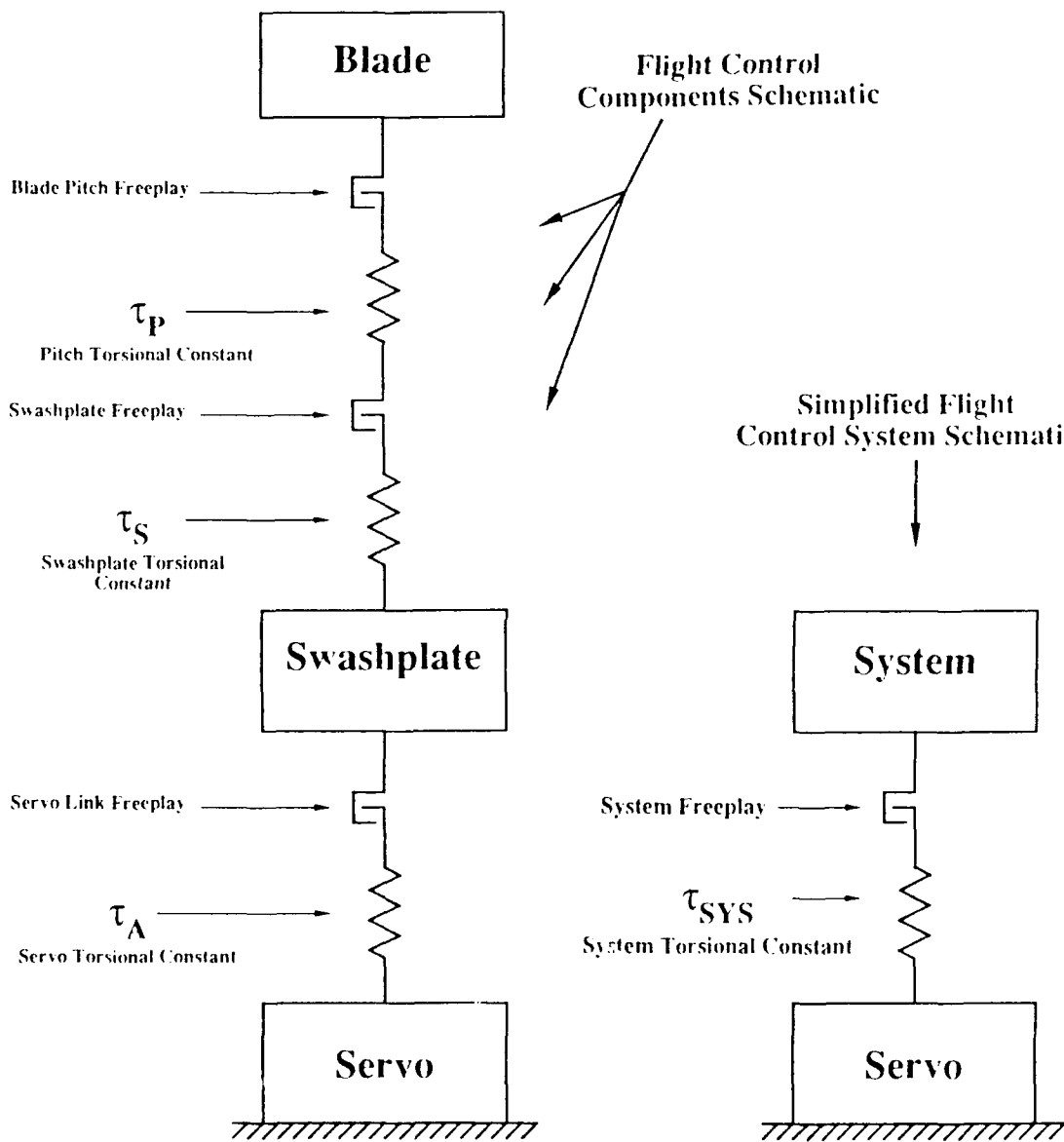


Figure 19. Flight Control Spring and Freeplay Representation

1. Servo Actuator Assembly

The servo actuator assembly's spring constant was determined by disconnecting the actuator link from the swashplate and then applying a load to the link using a lever. This technique is presented schematically in Figure 20. The servo actuator, controlled by the radio system, attempted to hold a set position as the load was applied. Force on the servo was generated by applying weights incrementally to the lever. The force to the actuator link was twice the weight applied because of the moment arm lengths about the fulcrum. Linear motion of the actuator link was measured using a pointer, fixed to the link, and referenced to a stationary ruler. Data attained from this measurement technique was converted to units compatible with the blade pitch angle, thereby giving a torsional constant

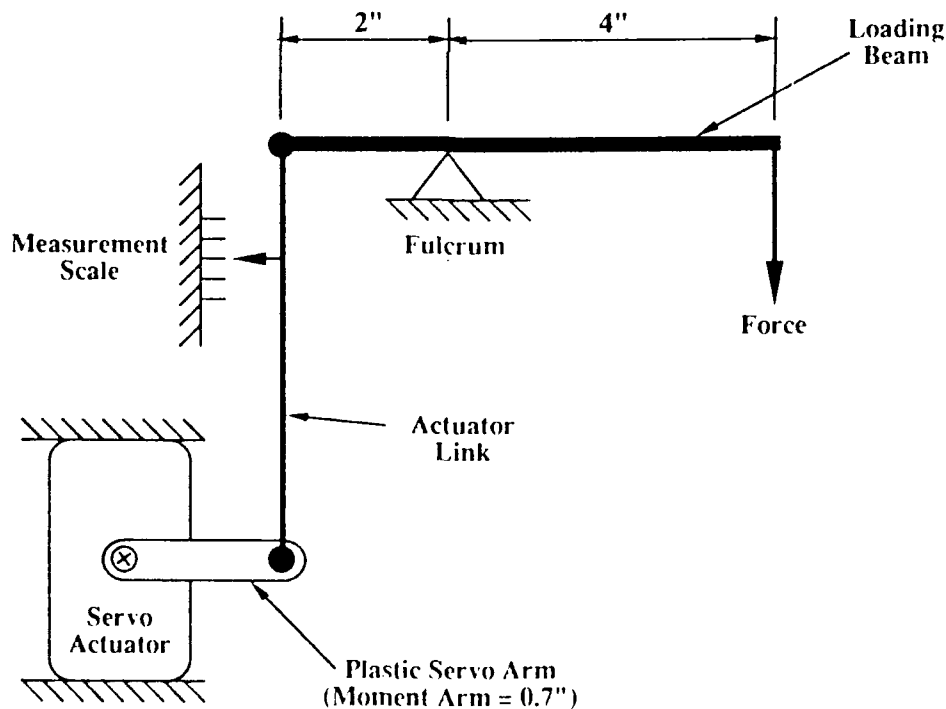


Figure 20. Servo Loading Schematic

associated with the servo actuator (τ_A). The fulcrum method facilitated loading in only one direction. It is assumed that the servo torsional constant is constant for an oppositely applied loading.

2. Blade Pitch Link and Pitch Horn Assembly

To measure the torsional constant for the blade pitch link and pitch horn assembly (blade pitch torsional constant, τ_P), it was necessary to maintain the swashplate assembly in a fixed position. This was accomplished by fashioning a clamping arrangement which, when tightened, securely held the swashplate to two hardwood blocks placed underneath it. This clamp arrangement is seen from a side view in Figure 21. With the swashplate secured, a torque was applied to the blade

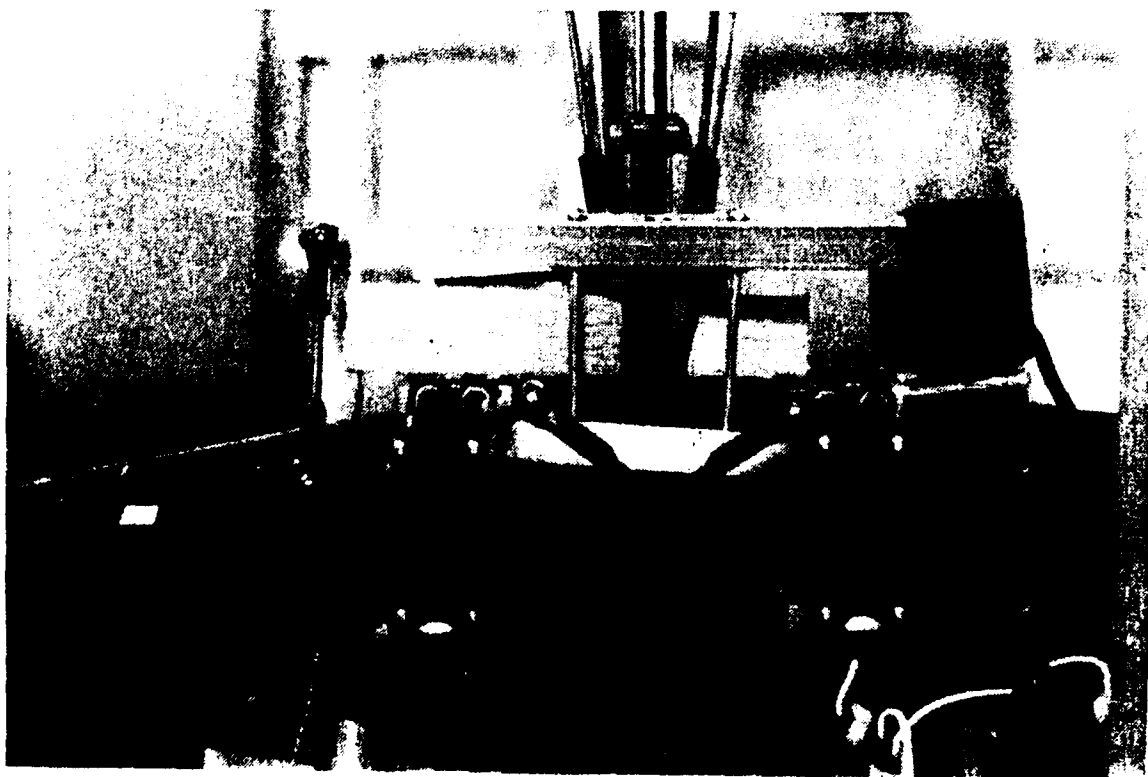


Figure 21. Swashplate Clamp Arrangement

grip using a cantilever beam inserted in the blade grip perpendicular to the blade pitch axis. Torque was generated by applying weight incrementally to the cantilever at a known moment arm. This process is shown schematically in Figure 22. Blade pitch angle changes were read directly from a pitch gauge inserted in the blade grip and referenced to a fixed mark, as seen in Figure 23.

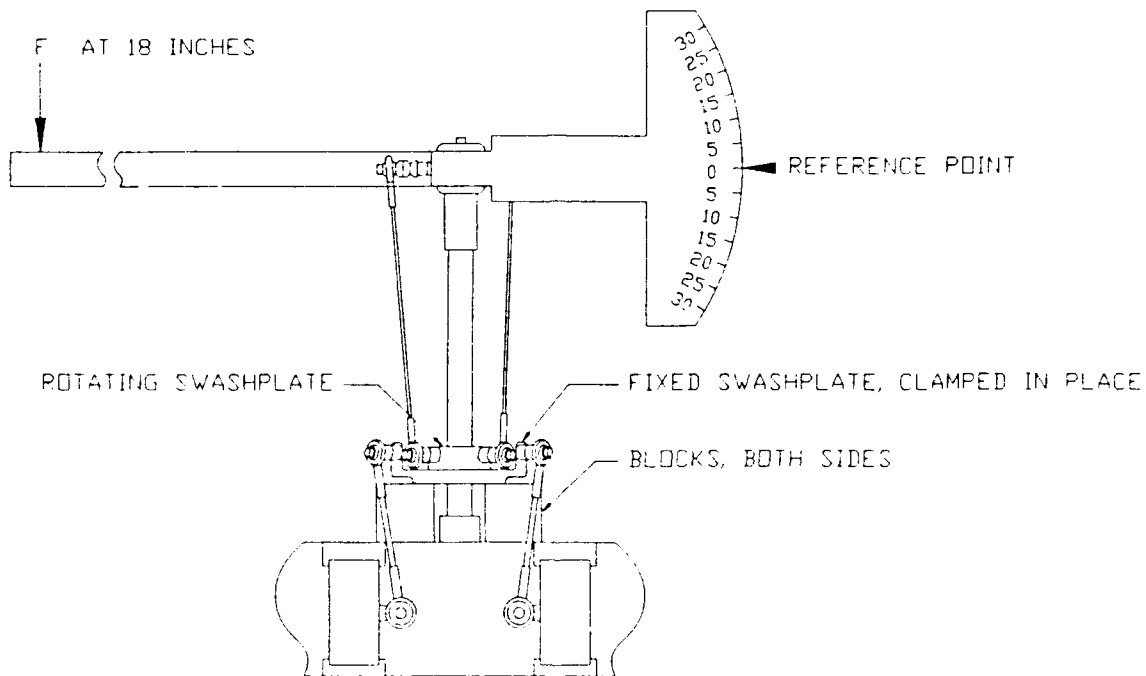


Figure 22. Pitch Torsional Constant Loading Schematic

3. Total System

The total system torsional constant (τ_{SYS}) was measured with all linkages reconnected, the swashplate free to move, and the radio control system controlling the servos. The swashplate was set to a neutral position with the cyclic centered and the collective at approximately half pitch. The rotating system was positioned so



Figure 23. Blade Pitch Gauge

that the loaded blade's pitch link ball end on the rotating swashplate was directly over a ball link from either the pitch or roll servo. This alignment insured that only one pair of servos opposed the rotation of the swashplate caused by the torque applied to the blade. When alignment was established, the blade was loaded and measurements were taken in a manner similar to that use to measure τ_p . Torque was applied to only one blade at a time and reversing the cantilever allowed the torque to be applied in a negative sense. Torque was applied for the roll and pitch axis of the swashplate, allowing the servo pairs to be loaded independently.

4. Comparison of Individual Spring Constant Data

With the values of τ_A , τ_P and τ_{SYS} known, the torsional constant for the swashplate, τ_S , could be determined using superposition. The following equation was utilized:

$$\frac{1}{\tau_{SYS}} = \frac{1}{\tau_A} + \frac{1}{\tau_P} + \frac{1}{\tau_S} \quad (1)$$

which, when solved for τ_S takes the form:

$$\tau_S = \left(\frac{1}{\frac{1}{\tau_{SYS}} - \frac{1}{\tau_A} - \frac{1}{\tau_P}} \right) \quad (2)$$

B. BLADE FLAPPING HINGE TORSIONAL CONSTANT

To measure the blade flapping torsional constant (τ_F) it was necessary to secure the swashplate as done for the τ_P measurements. A cantilever arm was inserted into the blade grip with its centerline coincident with the blade pitch axis. Torque was generated by applying weights incrementally at a known moment arm from the flap axis. A dial indicator, secured to the airframe, was positioned under the blade retaining bolt (see Figure 24). This indicator displayed the linear motion of the blade retaining bolt about the flap axis, which was converted to a flap angle.

C. HHC ACTUATION POWER REQUIREMENTS

A preliminary estimate of the power required for HHC actuation was completed to ascertain the requirements of suitable actuators. An arbitrary HHC blade pitch amplitude of one degree was chosen since most reports indicate only small blade pitch inputs are required [Ref. 6:p. 4]. Normal Ω for the RPH is 1,100 rpm with the maximum Ω at approximately 1,300 rpm. Calculations were completed for Ω of 1,200 rpm, or 20 Hz. For the four-bladed rotor system, the 4Ω actuation frequency required for HHC inputs was 80 Hz. This frequency

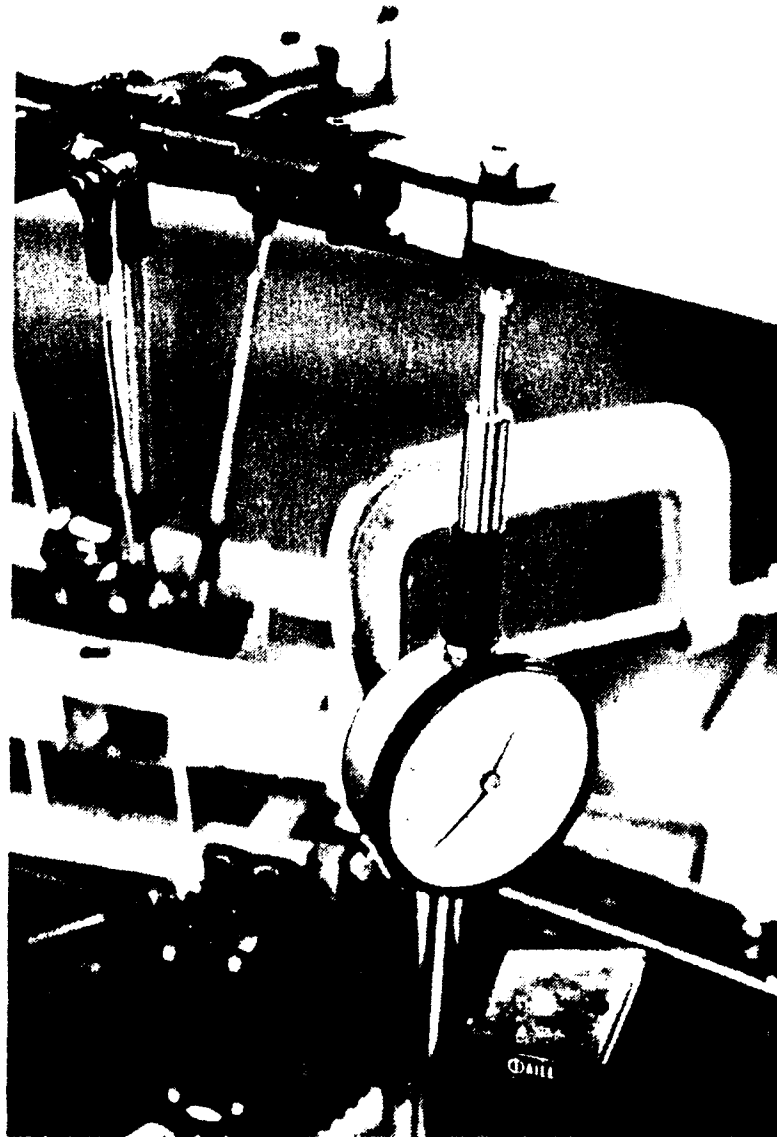


Figure 24. Dial Indicator Used for Blade Flapping Measurements

established the angular acceleration (α) required of the blade about its pitch axis. The following equations of simple harmonic motion were utilized for blade pitch:

Angular Displacement: $\theta = A \cos(4\Omega t + \varphi)$ (3)

Angular Velocity: $\omega = \frac{d\theta}{dt} = -4\Omega A \sin(4\Omega t + \varphi)$ (4)

Angular Acceleration: $\alpha = \frac{d\omega}{dt} = -(4\Omega)^2 A \cos(4\Omega t + \varphi)$ (5)

where A is the amplitude of the blade pitch angle, t is time, and φ is the phase constant. Setting φ to zero, the maximum blade pitch occurs at t equal to zero. Since the maximum acceleration (α_{MAX}) occurs at a phase shift of 180° from the maximum displacement, the absolute value of α at t equal zero is equal to α_{MAX} . The next step was to determine the mass moment of inertia of the rotor blade about its center of gravity. This was determined by treating the blade cross-section as two simple elements, a rectangular and triangular. These elements are depicted in Figure 25.

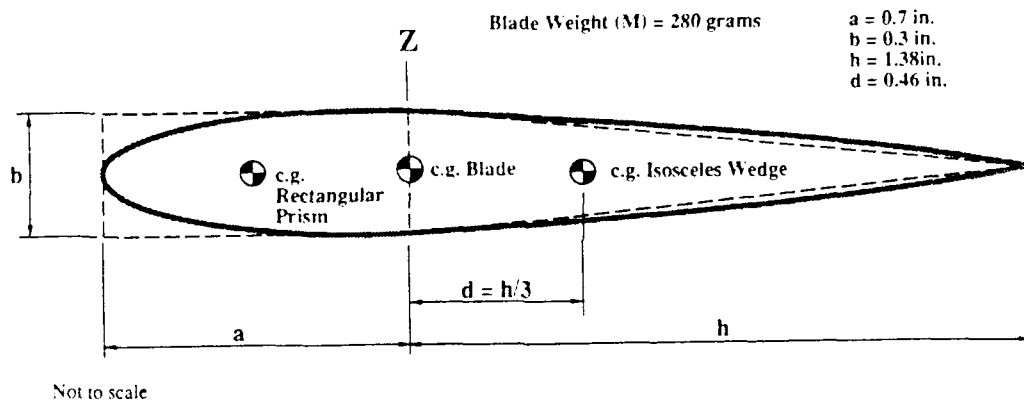


Figure 25. Blade Cross-Sectional Representation

In three dimensional space, the equation for mass moment of inertia of the rectangular prism about the blade's center of gravity is [Ref. 12]:

$$I_{Z_R} = \frac{1}{12}m(4a^2 + b^2) \quad (6)$$

where m is 1/2 of the mass (M) of the blade. The equation for the mass moment of inertia of the isosceles wedge [Ref. 13], corrected to the center of gravity using the parallel-axis theorem is:

$$I_{Z_W} = \frac{1}{72}m(4h^2 + 3b^2) + md^2 \quad (7)$$

The final mass moment of inertia for the entire blade about its center of gravity is:

$$J_B = I_{Z_R} + I_{Z_W} \quad (8)$$

With α_{MAX} and J_B known, the torque required to provide HHC pitch oscillation was obtained using the equation:

$$T_{MAX} = \alpha_{MAX} J_B \quad (9)$$

VII. RESULTS

A. CONTROL SYSTEM FREEPLAY AND TORSIONAL CONSTANTS

1. Servo Actuator Assembly

Data obtained from servo loading is contained in Table 3, along with calculated data which has been converted from servo displacement to blade pitch

TABLE 3. Servo Torsional Constant Data

Linear Force (oz.-force)	Linear Deflection (in.)	Torque (oz. in.)	Servo Angular Deflection (degrees)	Torque Applied to Blade (oz. in.)	Blade Angular Deflection (degrees)
11.64	0.000	8.15	0.000	16.30	0.00
23.49	0.006	16.44	0.491	32.89	0.30
32.95	0.014	23.06	1.146	46.12	0.71
37.74	0.020	26.42	1.637	52.84	1.01
42.40	0.025	29.68	2.045	59.36	1.27
46.77	0.030	32.74	2.454	65.48	1.52

angular deflection. The servo actuator's arm was 0.7 inches long. This moment arm was used to determine a servo torque value. An effective gear ratio existed between the servo arm's motion and the resulting blade deflection. This linear relation was 1.0° of blade rotation for every 1.61° of servo rotation. The value of torque applied to the blade is the result of two servos' action, assuming either a roll or pitch input, and is therefore twice the torque produced by an individual servo. Figure 26 shows the plotted data. The slope of the line is equal to the effective servo torsional constant, τ_A , and is approximately 25.5 oz. in./deg. The servo freeplay is indicated by the offset of the x-axis intercept from zero. The total servo freeplay corresponds to approximately one degree of blade pitch rotation. The

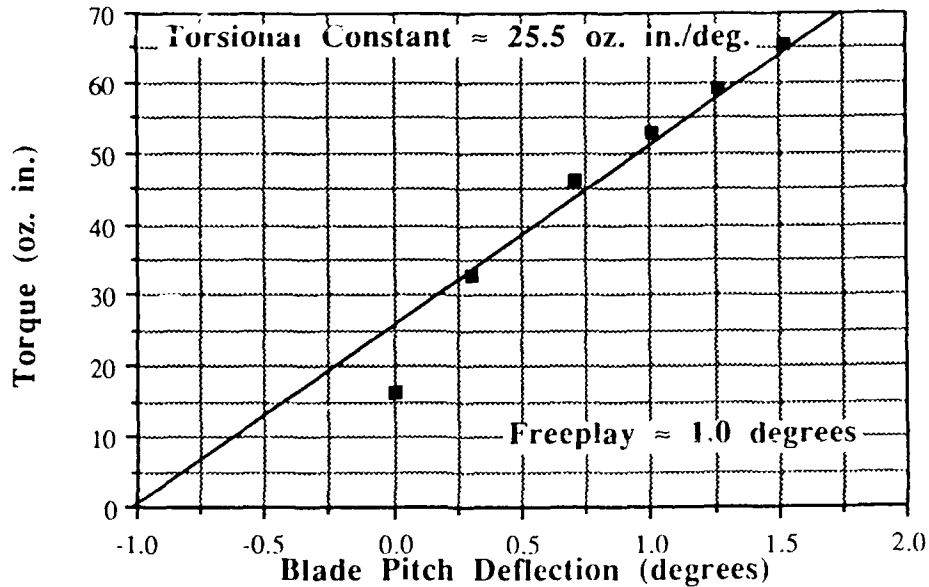


Figure 26. Servo Torsional Constant

plotted data indicates that the original assumption of linearity for the torsional constants is invalid. During loading of the servo, it was evident that the plastic servo actuating arm was deforming under the load applied. The value of freeplay suggested by the linear torsional constant, while inaccurate due to the function's nonlinearity, suggests a large amount of freeplay. This freeplay was noted during loading.

2. Blade Pitch Link and Pitch Horn Assembly

Data obtained for τ_p is presented in Table 4, along with the calculated torque and average blade deflection. Torque was computed using a cantilever moment arm of 18 inches. The slope of the plotted torque and average blade deflection data, seen in Figure 27, determined the value of τ_p . During data acquisition, it was noted that the rotor head appeared to be "tight" and allowed

TABLE 4. Blade Pitch Torsional Data

Applied Force (oz.-force)	Torque (oz. in.)	Blade Pitch Angle (degrees)				Average Blade Deflection (degrees)
		Blue	Green	Red	Yellow	
0.56	10.16	0.25	0.25	0.25	0.25	0.250
2.33	41.90	0.50	0.50	0.50	0.50	0.500
7.44	133.97	1.25	1.25	1.20	1.25	1.238
12.56	226.03	1.80	1.75	1.75	2.00	1.825
16.26	292.70	2.50	2.50	2.50	2.50	2.500

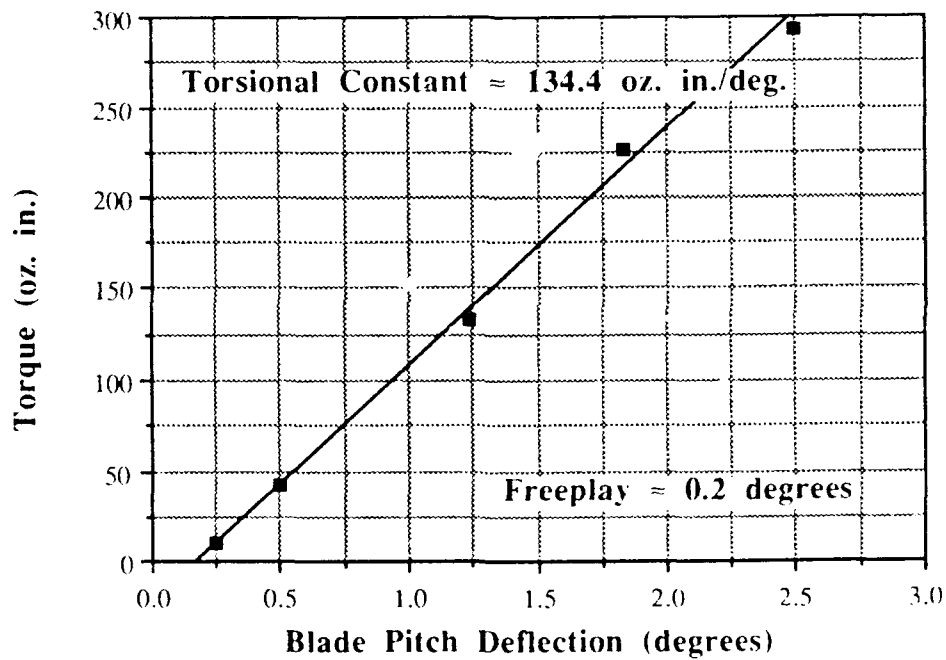


Figure 27. Blade Pitch Torsional Constant

for very little freeplay. This was confirmed by the plotted data with τ_p of approximately 134.4 oz. in./deg. and freeplay of approximately 0.2°.

3. Total System

The data for τ_{SYS} is shown in Table 5. The moment arm used for the cantilever was 18 inches. Data was obtained for both the roll and pitch servo pairs. This data is plotted in Figure 28. τ_{SYS} has been determined as an average of the slopes from both the roll and pitch servo loadings. The average slope gave a torsional constant for the system of approximately 59 oz. in./deg. with a freeplay of approximately 1.4°. The values appear to be adversely affected by the servo actuator's effect on the system.

TABLE 5. Total System Torsional Constant Data

Applied Force (oz.-force)	Torque (oz. in.)	Roll Servo Loading Blade Pitch Angle (degrees)	Pitch Servo Loading Blade Pitch Angle (degrees)
0.56	10.16	0.75	0.75
1.94	34.92	1.25	1.50
3.21	57.78	1.75	1.80
4.83	86.98	2.25	2.00
6.10	109.84	2.75	2.50
8.43	151.75	3.50	3.10
10.41	187.30	4.00	3.60
12.38	222.86	4.50	4.25
-0.56	-10.16	-0.75	-0.75
-1.94	-34.92	-1.25	-1.00
-3.21	-57.78	-1.75	-1.50
-4.83	-86.98	-2.50	-2.25
-6.10	-109.84	-2.75	-2.50
-8.43	-151.75	-3.50	-3.10
-10.41	-187.30	-4.00	-3.80
-12.38	-222.86	-4.50	-4.10

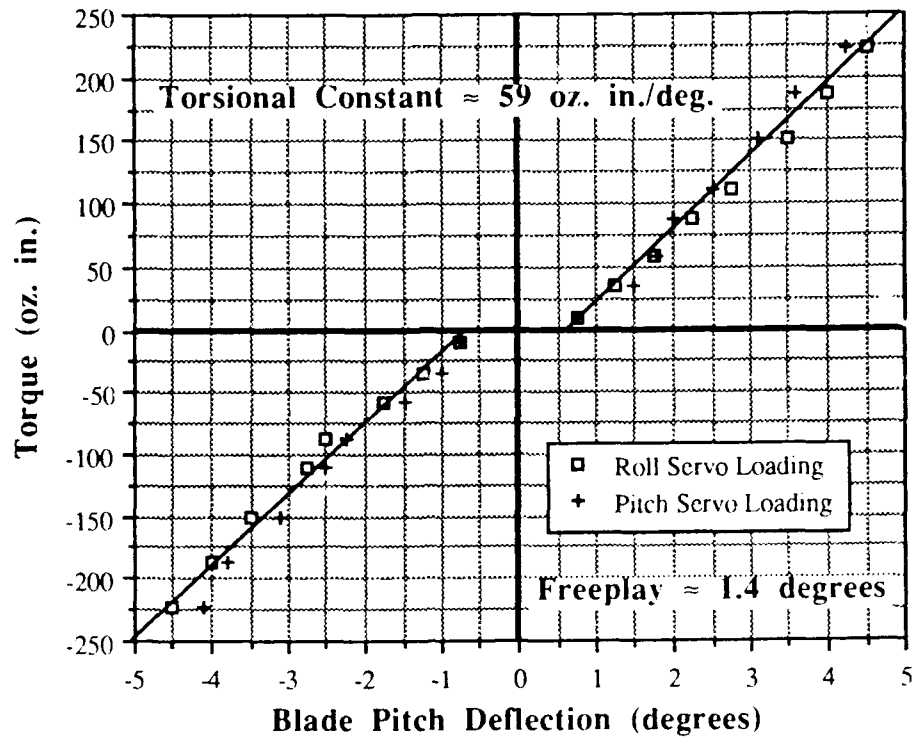


Figure 28. Flight Control System Torsional Constant

4. Comparison of Individual Torsional Constant Data

Table 6 shows the collective data which represents the individual torsional constants for the system. The positive loading data for the roll actuators has been

TABLE 6. Individual Spring Constant Data

Servo Torque (oz. in.)	Blade Angular Deflection (degrees)	Pitch Torque (oz. in.)	Blade Angular Deflection (degrees)	System Torque (oz. in.)	Blade Angular Deflection (degrees)
16.30	0.00	10.16	0.25	10.16	0.75
32.89	0.30	41.90	0.50	34.92	1.25
46.12	0.71	133.97	1.24	57.78	1.75
52.84	1.01	226.03	1.83	86.98	2.25
59.36	1.27	292.70	2.50	109.84	2.75
65.48	1.52			151.75	3.50
				187.30	4.00
				222.86	4.50

used for the total system data representation. This data has been displayed graphically in Figure 29 for comparison. This comparison of the different curves

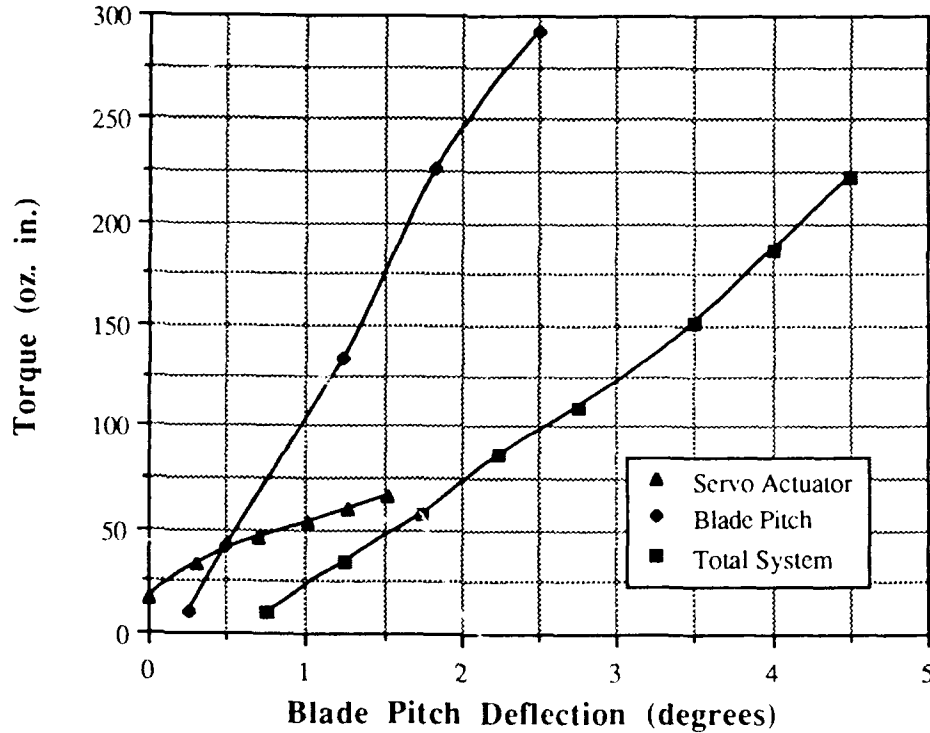


Figure 29. Comparison of Individual Torsional Constants

demonstrates two important points. First, it shows that the servo actuators were not loaded to a level high enough to compare with the other components. Secondly, it further emphasizes the nonlinearity of the data attained from the servo loading. When equation (2) is utilized to calculate τ_S , a value of -33.7 oz. in./deg. is attained. The fact that the value is negative illustrates the error in this methodology. Since the weakest torsional constant of the system is τ_p , the value for τ_{SYS} must be lower. While this methodology was not successful in returning a value for τ_S , the investigation has led to an important realization concerning the current control system. The servo actuators torsional constant value is too low to support the high

dynamic frequencies involved with HHC actuation. A large majority of the HHC actuation would be absorbed in the spring action of the actuator and its servo arm.

B. BLADE FLAPPING HINGE TORSIONAL CONSTANT

Data attained for the blade flapping hinge torsional constant is shown in Table 7. The moment arm used for the cantilever was 12 inches and the dial

TABLE 7. Flap Hinge Data

Applied Force (oz.-force)	Torque (oz. in.)	Deflection at Dial Indicator (in.)	Flap Angle (Degrees)
6.6	79.15	0.024	0.44
12.03	144.34	0.055	1.00
16.47	197.67	0.080	1.45
17.95	215.45	0.087	1.58
23.39	280.63	0.112	2.04
27.83	333.97	0.125	2.27

indicator measurements were taken at a distance of 3.15 inches from the flapping hinge. The deflection of the blade grip assembly, about the flapping hinge was computed using the arctangent of the dial indicator deflection over 3.15 inches. The data has been graphically presented in Figure 30 and demonstrates a τ_F of approximately 135 oz. in./deg. with freeplay at approximately 0.1°.

C. HHC ACTUATION POWER REQUIREMENTS

Utilizing equations (3), (4), and (5), the values for 1.5 cycles of the blade pitch oscillations were calculated and plotted (See Figure 31). With 1.0° of total blade pitch at a frequency of 80 Hz (502.56 rad/sec), α_{MAX} equals 2,204.9 rad/sec². From equation (6), (7), and (8), the following values were computed:

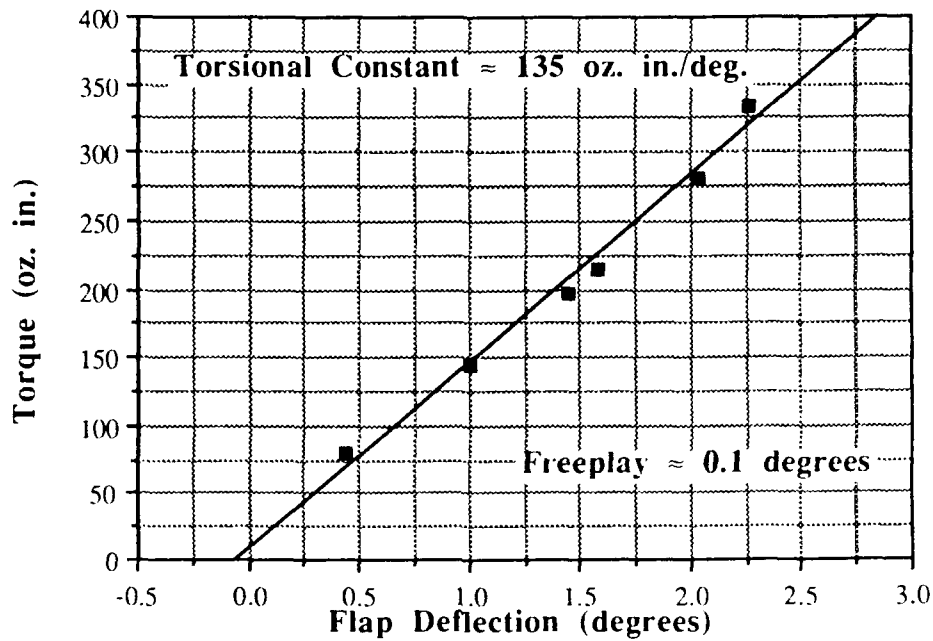


Figure 30. Rotor Blade Flapping Torsional Constant

$$I_{Z_R} = 0.0022 \text{ oz. in. sec.}^2$$

$$I_{Z_W} = 0.0041 \text{ oz. in. sec.}^2$$

$$J_B = 0.0063 \text{ oz. in. sec.}^2$$

With the value of α_{MAX} and J_B known, equation (9) was used to compute the maximum torque required to provide 1° of HHC blade pitch motion at 80 Hz. T_{MAX} was computed to be 13.89 oz. in. This value is only valid for acceleration of the blade section and does not contain the mass moment of inertia of the actuator. Therefore, a specific actuator must be considered. An actuator which can provide the acceleration required for HHC and also the normal flight control actuation is a

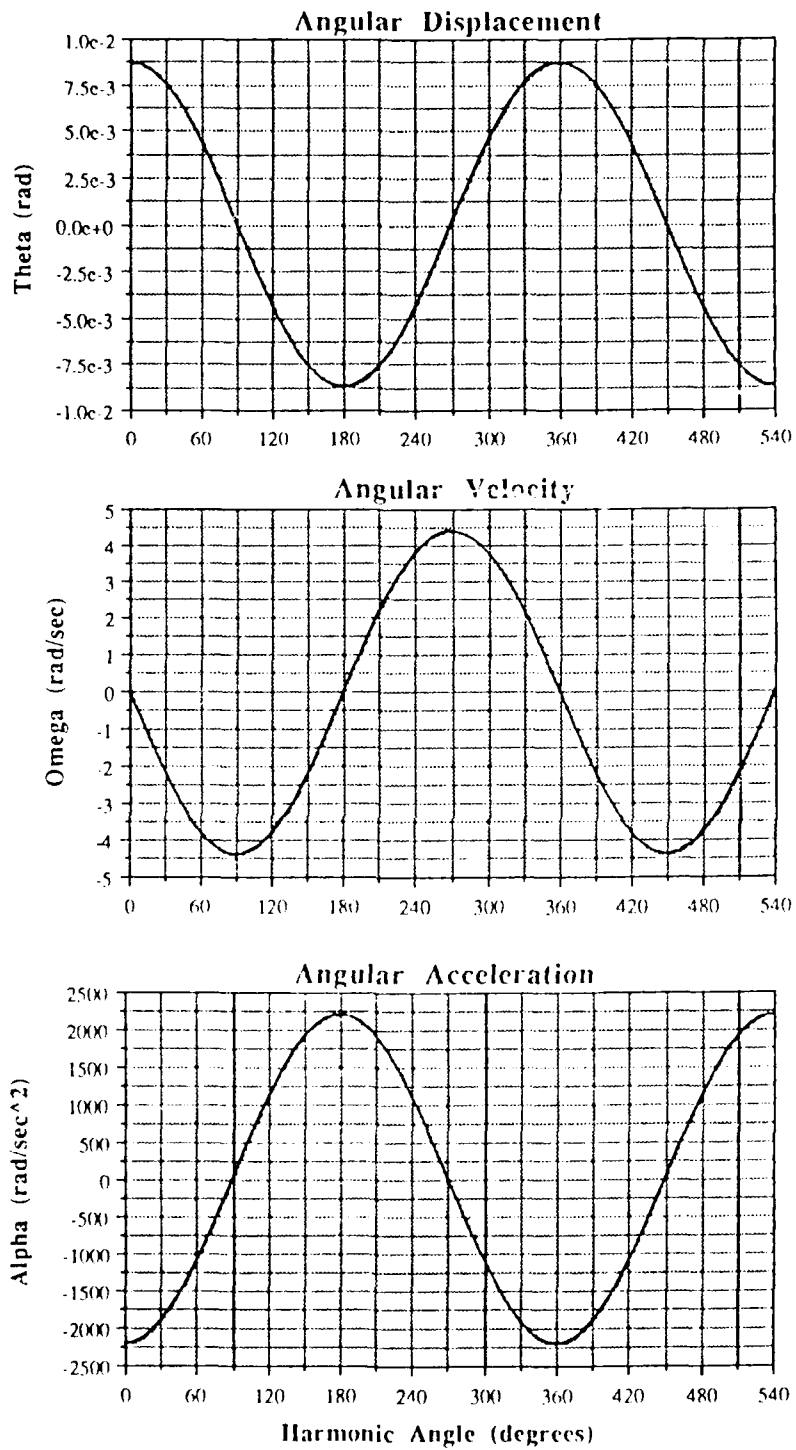


Figure 31. Blade Pitch Characteristics for 1.0° Blade Oscillation

brushless DC torque motor. The Vernitorq VBTM34-J was chosen as a representative motor. This motor is capable of providing a peak torque of 80 oz. in. and a continuous torque of 45 oz. in. It has a weight of 21.5 oz. and a rotor inertia (J_M) of 0.0084 oz. in. sec². By adding J_B to J_M , the total inertia of the blade and the motor is found (J_T). The value for J_T is 0.0147. Substituting J_T for J_B in equation (9), a T_{MAX} of 32.4 oz. in. is attained. This value is well within the capability of the chosen torque motor. It must be remembered that this T_{MAX} value only represents the torque required to provide HHC actuation. It does not account for normal flight loads. For this reason, a torque motor with a conservatively high T_{MAX} value was chosen as the representative motor.

VIII. CONCLUSIONS AND RECOMMENDATIONS

A. CONCLUSIONS

The goal of this research effort was the establishment of a remotely piloted helicopter flight test program for the study of higher harmonic control. This goal is the first stage of the Department of Aeronautics and Astronautics' overall goal of acquiring an inhouse asset capable of generating HHC flight test data. Several steps, which define the establishment of the RPH test flight program, have been accomplished during this research effort. These steps included the determination of attributes required of a RPH used for HHC studies, the selection and acquisition of an RPH capable of completing the intended mission, and the preliminary analysis for modification of the RPH to an HHC configuration. Further work, to continue toward the overall department goal, has been undertaken by two follow-on students.

Determination of the attributes required of an RPH yielded three major requirements which had to be met. These requirements were: (1) a four-bladed rotor head; (2) payload capacity of approximately 15 pounds; and (3) a total system cost no greater than \$10,000. While other stipulations to the RPH were considered to be important, these three specific requirements were the most crucial to the overall goal. Acquisition of an RPH capable of meeting the determined requirements was then accomplished. Following acquisition, RPH support requirements such as laboratory facilities, RPH flying sites, and qualified RPH pilots were addressed. Of the support requirements, the solicitation of a suitable RPH pilot may be the hardest to accomplish. The pilot chosen must have extensive

RPH experience and must be available for test flights in the local area. The possibility of acquiring funding to remunerate a qualified RPH pilot must be considered if no qualified local pilots, willing to donate their time and piloting expertise, can be found.

The preliminary analysis of the current RPH flight control system has demonstrated two major points: (1) flight control modification is necessary to alter system freeplay and torsional constant values; and (2) motors, capable of generating HHC actuation of the rotor blades, are available. While the modification of the flight control system was expected from the programs inception, the analysis has shown that the servo actuators represent the largest amount of freeplay and weakest torsional constant. Since these servos were incapable of providing the necessary HHC actuation, the incorporation of new HHC actuators must address the design considerations of freeplay and torsional constants. The new actuators chosen should be designed with minimum freeplay and a value of stiffness greater than the other components in the flight control system. Calculations completed for the torque requirements of HHC actuators showed that brushless DC torque motors are available which are capable of HHC actuation. These preliminary calculations were performed with only the inertia of the blade and torque motor considered. Further calculations, to include the inertias of the associated control linkages and freeplays, must be completed as the new control system is designed. These calculations will be possible only after the anticipated flight control components have been defined.

B. RECOMMENDATIONS

Continued work on the HHC flight control system is required. The preliminary calculations performed for the flight control system are only a starting

point for the HHC control system definition. As design continues, redefinition of the anticipated actuation system's freeplay and torsional values must be accomplished. Concurrent with the flight control system definition, an actuator controlling system should be designed. This controlling system should be integrated with the current radio control system to allow for operation with or without HHC actuation. The anticipated open loop control system should be designed with a fail-safe capability, so that the HHC actuation can be deselected at any time during operation. The fail-safe operation should protect the RPH from possible actuator hardovers or extraneous signals caused by an HHC system failure. The control system should also be designed with the ability to be modified to a closed loop controller format for future research.

Another area which will require work is the integration of a system capable of monitoring the RPH's vibration and performance. Incorporation of accelerometers will be required to monitor vibration. Monitoring of performance attributes is more challenging since no clear means of measuring engine power output or torque has been identified. A methodology for determining these performance values must be formulated. Other areas of possible interest for instrumentation are the stresses and motions of the rotor blades in flight. With all the proposed instrumentation, some means of either onboard data recording or telemetry must be devised. All instrumentation and data recording devices must be designed with minimum weight as a major consideration, due to the payload constraints of the RPH.

As mentioned previously, the recruitment of a suitable RPH pilot requires further effort. The most promising possibility lies in the hiring of a UAV

technician for the UAV lab. With the proper training, the UAV technician would be a valuable piloting asset. Also, further work on the UAV lab itself is required.

Prior to any actual flight test work, a methodology for flight testing the RPH must be carefully formulated. It must be realized that the RPH is an actual aircraft which requires careful preparation and extreme care to fly. Development of specific guidelines which ensures that the flight test program is conducted safely and effectively is required. This program should be designed to protect the RPH from any conceivable problems which may cause a mishap. Liaison with the personnel at the Rotary Wing Test Directorate at the Naval Air Test Center in Patuxent River, Maryland may be extremely helpful to accomplish this task.

Another area which may be pursued is modeling of the RPH fuselage and rotor system in a finite element program such as DYSCO (available at the NPS). This would allow the researcher to obtain solutions such as eigen-analysis, frequency response, and time histories for the mathematical model defined. This would be useful when alterations to the rotor system or fuselage are considered. By redefining the mathematical model of the component to be altered, an insight into the effect of the change on the RPH would be obtained.

Appendix

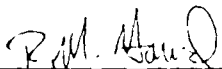
MEMORANDUM OF UNDERSTANDING

BETWEEN

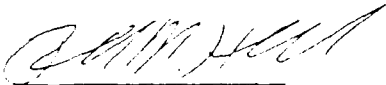
COMMANDER, FRITZSCHE ARMY AIRFIELD AND NAVAL POSTGRADUATE SCHOOL

SUBJECT: Remotely Piloted Vehicle Operations at Fritzsche AAF.

1. All remotely piloted vehicle (RPV) operations at Fritzsche AAF (FAAF) shall be conducted in accordance with paragraph 9-7: AR 95-2, Air Traffic Control, Airspace, Flight Activities and Navigational Aids. (enclosure)
2. The Operations Officer, FAAF shall be notified no later than 72 hours prior to the planned flight. Operations shall notify FAAF Crash station of the date and time of any scheduled RPV operations. If RPV operations are conducted when the control tower is in operation, coordination between Operations and ATC shall be accomplished as soon as practicable after notification. Operations shall disseminate applicable NOTAMs as required.
3. Personnel operating RPVs shall remain in constant radio contact with the Air Traffic Control tower, or, if the tower is closed, Base Operations via Motorola Walkie Talkie. The Motorola shall be provided by FAAF Operations, Building 518.
4. Normal FAAF aircraft operations shall receive priority over RPVs. RPV operations shall not delay or disrupt normal air traffic operations at FAAF. Navy Flying Club aircraft should be requested to remain clear of the area while RPV operations are scheduled. RPV operations shall be halted prior to aircraft arriving or departing from FAAF. RPV operations may commence after an arriving aircraft has parked, or a departing aircraft has reported at least 2 nautical miles from the airfield, or clear of the Control Zone.
5. RPVs shall remain within 2 nautical miles of FAAF at all times. No flights are permitted south of runway 29/11, or south of the runway extended centerline. No flight within 1 nautical mile of the city of Marina is authorized. No flights are authorized between official sunset and official sunrise. No flights are authorized if the Crash Crew is off the airfield.
6. RPV operators assume all responsibility for compliance with: this MOU, AR 95-2, and all damage incurred as the result of RPV operations.
7. POC is Joe White 242-3260/5706.


DR. RICHARD M. HOWARD
PHD, Faculty Advisor
Naval Postgraduate School

DATE: 1 MAR 90


RONALD M. HOLLAND
LTC, AV
Commander, Fritzsche AAF

DATE: 1 MAR 90

9-7. Remotely piloted vehicles (RPVs)

a. RPV operations will be rigidly controlled to avoid hazards to other air traffic. The following restrictions apply to RPV operations:

(1) Flights will be conducted within restricted areas that have been approved for RPV operations. In addition, RPV operations may be conducted within positive control airspace (PCA), provided it has been properly coordinated with FAA; and within warning areas, provided it has been properly coordinated with the Department of the Navy and the FAA.

(2) Outside the above areas, with the exception of (b) below, RPVs must be accompanied by a chase plane with direct communications with the controlling source facilities. The chase plane pilot will ensure the RPV is maneuvered to avoid potential conflicts, either by having control of the

RPV or by relaying instructions to the controlling source. The concerned FAA region may approve alternate means of observing RPV flight and communicating with the controlling source when they provide a level of safety equal to that of the chase plane.

b. RPVs that may be classed as model aircraft such as the remotely controlled miniature target (RCMAT) may be operated as follows:

(1) The operating site should not be located near populated areas and avoid noise sensitive areas such as parks, schools, hospitals, churches, etc.

(2) Avoid operations in the presence of spectators until the RPV has been successfully flight tested and proven airworthy.

(3) RPVs will not be flown above 400 feet AGL.

(4) Operations will not be conducted within 3 miles of an airport/heliport without notifying the airport/heliport operator. When an air traffic facility is located at the airport/heliport, notify the control tower or flight service station.

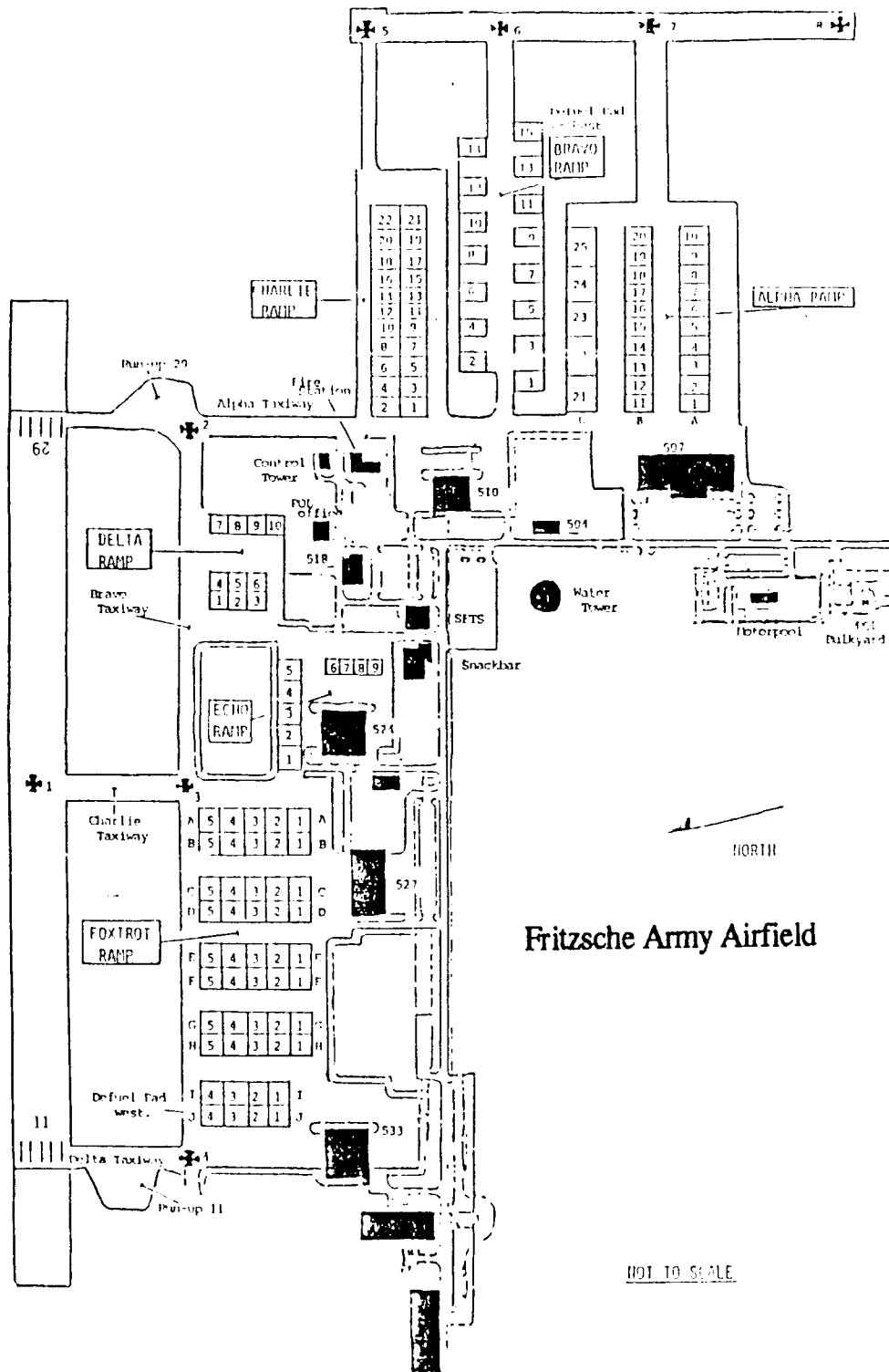
(5) Give right of way to, and avoid flying in proximity of, manned aircraft.

(6) Observers will be used to assist in avoiding nonparticipating aircraft.

(7) Each RPV and associated radio control equipment will be checked for normal operations prior to launch.

(8) Live fire exercises involving RPVs will be conducted within controlled firing areas (CFAs) or restricted areas. All rules and restrictions applicable to these areas apply.

c. For additional information or clarification, contact the appropriate DARR or the DA AT&A Manager.



Fritzsche Army Airfield

NOT TO SCALE

LIST OF REFERENCES

1. Walsh, D. M., "Flight Tests of an Open Loop Higher Harmonic Control System on an S-76A Helicopter," paper presented at the American Helicopter Society Forum, 42nd, Washington, D. C., p. 831, 2-4 January 1986.
2. AIAA, ASME, ASCE, AHS, and ASC, Structural Dynamics and Materials Conference, 30th, Technical Paper 89-1215, *Application of Higher Harmonic Control (HHC) to Hingeless Rotor Systems*, by K. Nguyen and I. Chopra, p. 507, 3-5 April 1989.
3. Chopra, I., "Notes on Helicopter Dynamics," Lecture notes from the Department of Aerospace Engineering at the University of Maryland, College Park, Maryland, p. 312, n.d.
4. Hall, S. R. and Werely, N. M., "Linear Control Issues in the Higher Harmonic Control of Helicopter Vibrations," paper presented at the American Helicopter Society Forum, 45th, Boston, MA, p. 957, 22-24 May 1989.
5. Sarigul-Klijn, M. M., Kolar, R., Wood, E. R., and Straub, F. L., "On Chaos Methods Applied to Higher Harmonic Control," paper to be presented at the American Helicopter Society Forum, 46th, Washington, D. C., pp. 1-21, May 1990.
6. Wood, E. R., Powers, R. W., Cline, J. H., and Hammond, C. E., "On Developing and Flight Testing a Higher Harmonic Control System," *Journal of the American Helicopter Society*, January 1985.
7. Gessow, A., and Myer, G. C., *Aerodynamics of the Helicopter*, Frederick Ungar Publishing Co., p. 309, 1985.
8. Johnson, W., *Helicopter Theory*, p. 696, Princeton University Press, 1980.
9. Harvey, D., "U.S. Defense: The Belt Begins to Tighten," *Rotor & Wing International*, v. 24, No. 1, p. 37, January 1990.
10. Telephone conversation between Mr. John Smith, Pacific RPV, Startup, WA, and the author, 14 March 1990.

11. Wood, E. R., "Review of Higher Harmonic Control System Load-Deflection Test Results," paper presented at NASA/Langley Research Center, Hampton, Virginia, 23 March 1982.
12. Beers, F. P., *Vector Mechanics for Engineers*, 3rd ed., p. 938, McGraw-Hill Book Company, 1977.
13. Litton Data Systems, *Engineering Design Manual*, p. 5-305, 25 January 1988.

INITIAL DISTRIBUTION LIST

	<u>No. of Copies</u>
1. Defense Technical Information Center Cameron Station Alexandria, Virginia 22304-6145	2
2. Library, Code 0142 Naval Postgraduate School Monterey, CA 93943-5000	2
3. Chairman, Code 67 Department of Aeronautics and Astronautics Naval Postgraduate School Monterey, CA 93943-5000	6
4. Professor R. M. Howard, Code 67 Ho Department of Aeronautics and Astronautics Naval Postgraduate School Monterey, CA 93943-5000	2
5. Mr. Rick Wooten Deputy Director UAV Program Development Directorate CMP PDA-14UDA Washington, D. C. 20361-1014	1
6. LT James G. Scott 591 Peabody Rd. #237 Vacaville, CA 95687	2
7. LT Charles Webb 1021 Halsey Dr. Monterey, CA 93940	1
8. Mr. John Smith Pacific RPV P. O. Box J Startup, WA 98293	1

9. Mr. Jerry P. Higman
NPS - SMC 1395
Monterey, CA 93943 1

10. LT J. J. McGovern
NPS - SMC 2513
Monterey, CA 93943 1